


 Cite this: *RSC Adv.*, 2025, **15**, 3192

 Received 10th November 2024  
 Accepted 10th January 2025

 DOI: 10.1039/d4ra07996e  
[rsc.li/rsc-advances](http://rsc.li/rsc-advances)

## Applications of catalytic systems containing DNA nucleobases (adenine, cytosine, guanine, and thymine) in organic reactions

 Zahra Khademi and Kobra Nikoofar \*

In recent years, nucleobases have attracted special attention because of their abundant resources and multiple interaction sites, which enable them to interact with and functionalize other molecules. This review focuses on the catalytic activities of each of the four main nucleobases found in deoxyribonucleic acid (DNA) in various organic reactions. Based on the studies, most of the nucleobases act as heterogeneous catalytic systems. The authors hope their assessment will help chemists and biochemists to propose new procedures for utilizing nucleobases as catalysts in various organic synthetic transformations. The review covers the corresponding literature published till the end of August 2023.

### 1. Introduction

Nucleobases, such as adenine (A, 1), guanine (G, 2), cytosine (C, 3), thymine (T, 4), and uracil (U, 5), are the fundamental units of the genetic code and have been found in DNA (Scheme 1). Nucleosides are made up of a sugar ring (2'-deoxyribose for DNA and ribose for RNA) and a nucleobase. Nucleotides contain a nucleoside and at least one phosphate unit.

The bases A, T, C, and G are found in deoxyribonucleic acid (DNA), while A, U, C, and G are present in RNA. It is widely known that A binds to T (or U), while G pairs with C through hydrogen bonding. Due to the capability of nucleobases to form base pairs and stack upon one another, they are capable of forming long-chain helical frameworks, such as those found in DNA and RNA.<sup>1–4</sup> Overall, the nucleobases can interact with each other as well as with other organic/inorganic small molecules.<sup>1</sup>

Adenine and guanine have a fused-ring structure derived from purine; thus, they are classified as purine bases. On the other hand, cytosine, uracil, and thymine consist of a simple heterocyclic aromatic ring derived from pyrimidine, and hence, they are called pyrimidine bases.<sup>5,6</sup>

Adenine was first synthesized as a white powder by Oro in 1960.<sup>7</sup> This compound was produced by heating concentrated ammonium cyanide ( $\text{NH}_4\text{CN}$ , 1–15 M) at 27 °C to 100 °C for several days, followed by the elimination of a black polymer through centrifugation and the reaction of the supernatant with HCl.<sup>8</sup>

Thymine was first isolated by Kossel and Neumann in 1893 from calf thymus glands, followed by its first synthesis through hydrolysis of the related nucleoside derived from natural

sources. In the early 1900s, Fischer presented a synthetic procedure starting from urea, but a more applicable method utilized methylisothiourea instead of urea in the condensation reaction with ethyl formyl propionate in water to form the pyrimidine intermediate, which was then subjected to acidic hydrolysis to afford thymine, with methanethiol as a by-product.<sup>9</sup>

In 1984, cytosine was isolated through the hydrolysis of calf thymus tissue. Its structure was identified in 1903, and it was first synthesized from 2-ethylthiopyrimidin-4(3H)-one.<sup>10</sup>

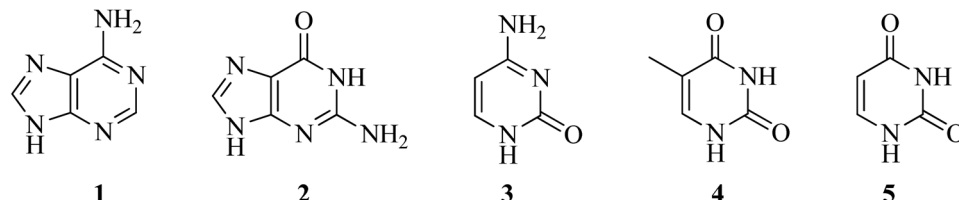
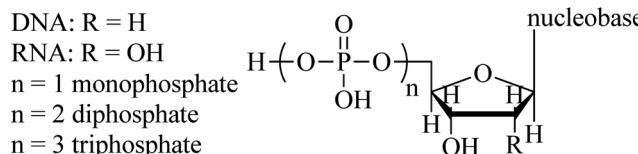
The first isolation of guanine was reported in 1846 by Unger from the excreta of sea birds as a mineral. Subsequently, between 1882 and 1906, the guanine structure was discovered, and the transformation of uric acid into guanine was revealed.<sup>11,12</sup>

Uracil was originally identified in 1900 by Ascoli and then isolated *via* hydrolysis of yeast nuclein.<sup>13</sup> This compound was also detected in bovine thymus and spleen.<sup>14</sup>

Because of the widespread utility of nucleobases, many studies have been published on different synthesis methods for nucleobases. For example, in 2022, Wang *et al.* prepared a nitrogen-doped carbon-based Co/Ni bimetallic catalyst (2 wt% Co/Ni@NC-700-10) using chitosan as the nitrogen and carbon source. It was found to be effective for guanine formation, utilizing 2,4-diamino-5-nitroso-6-hydroxypyrimidine (DANHP, 6) as starting material. In the first step, the reaction was initiated *via* the one-pot reductive *N*-formylation of 6 with formic acid (7) using 2 wt% Co/Ni@NC-700-10 in acetonitrile media at 150 °C to obtain 2,4-diamino-5-formyl-6-hydroxypyrimidine (DAFHP, 8) with excellent conversion (95.6%) and selectivity (97.6%), which after isolation underwent a cyclization reaction in the presence of formic acid (7) and sodium formate at 110 °C to achieve guanine (2). Based on the resulting HPLC spectra, the

Department of Organic Chemistry, Faculty of Chemistry, Alzahra University, P.O. Box 1993891176, Tehran, Iran. E-mail: [k.nikoofar@alzahra.ac.ir](mailto:k.nikoofar@alzahra.ac.ir); [kobranikooft@yahoo.com](mailto:kobranikooft@yahoo.com); Fax: +982188041344; Tel: +982188041344





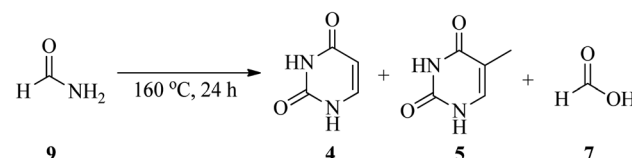
Scheme 1 Structures of nucleobases, nucleosides, and nucleotides.

conversion of **8** was about 100% with an excellent selectivity of 97.9% (Scheme 2).<sup>15</sup>

In 2021, an article entitled “Prebiotic route to thymine from formamide-a combined experimental-theoretical study” focused on the catalyst-free conversion of uracil to thymine through the thermolysis of formamide (**9**) at 160 °C within 24 h. This reaction progressed in the presence of formic acid (**7**) as a key molecule formed *via* the hydrolysis of **9** (Scheme 3). It is important that the disproportionation of formic acid (**7**) resulted in the formation of CO<sub>2</sub> and formaldehyde (**10**), and the latter compound plays an essential role in the hydroxymethylation of uracil<sup>16</sup> in the first step of the transformation procedure. The reaction was followed by the esterification of the hydroxyl group of 5-hydroxymethyluracil (**11**) to give **12**, which finally rearranged to thymine (**4**) upon the removal of CO<sub>2</sub> (Scheme 4).<sup>17,18</sup>

In 2020, Yadav *et al.* reported a review article entitled “Chemistry of abiotic nucleotide synthesis”, which pointed to the prebiotic synthesis of nucleobases from HCN derivatives, such as formamide and urea<sup>19</sup> or by other sources, with the exception of HCN and formamide.<sup>20</sup> In 2018, a review entitled “Origins of building blocks of life: a review” reported various methods for the synthesis of nucleobases under simulated prebiotic conditions.<sup>21</sup>

In addition to the above-mentioned methods, the nucleobases could be generated under various conditions. For example, the Nelson group in 2001 studied the synthesis of cytosine and uracil from urea and cyanoacetaldehyde at 100 °C

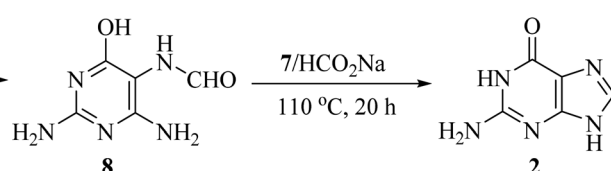
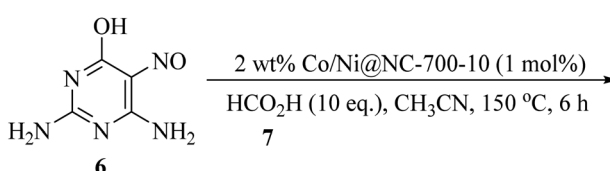


Scheme 3 Synthetic procedure for thymine.

under dry-down conditions and in solution at 4 °C and –20 °C.<sup>22</sup> In 2004, Orgel prepared adenine *via* the photochemical conversion of the tetramer of hydrogen cyanide in eutectic solution to 4-amino-5-cyano-imidazole.<sup>23</sup> Cleaves *et al.* in 2006 reported a simple prebiotic procedure to obtain cytosine and uracil upon freezing in solution.<sup>24</sup> Menor-Salván *et al.* in 2009 synthesized cytosine and uracil from cyanoacetylene/cyanoacetaldehyde and frozen urea solution under a methane/nitrogen atmosphere.<sup>25</sup> In 2007, they also obtained some purine bases through the spark activation of an atmosphere of methane, nitrogen and hydrogen in the presence of an aqueous aerosol.<sup>26</sup>

Formamide (which could be obtained from hydrogen cyanide and water) has received potential pre-genetic and pre-metabolic interest and is sometimes considered the origin of life.<sup>27</sup>

Owing to the critical role of formamide in the prebiotic synthesis of nucleobases, numerous studies have been performed utilizing formamide as a possible source of nucleobases

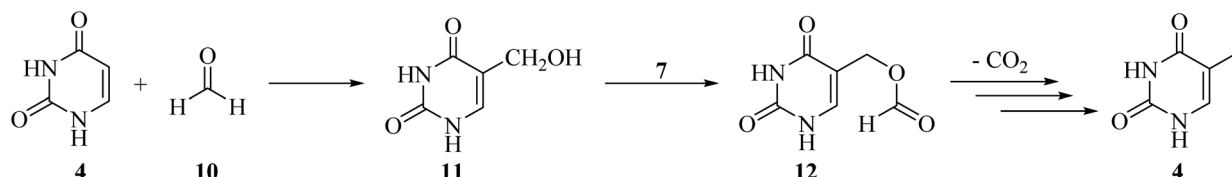


conversion: 95.6%  
 selectivity: 97.6%

conversion: ~ 100%  
 selectivity: 97.9%

Scheme 2 Synthetic procedure for guanine form DANHP and formic acid.



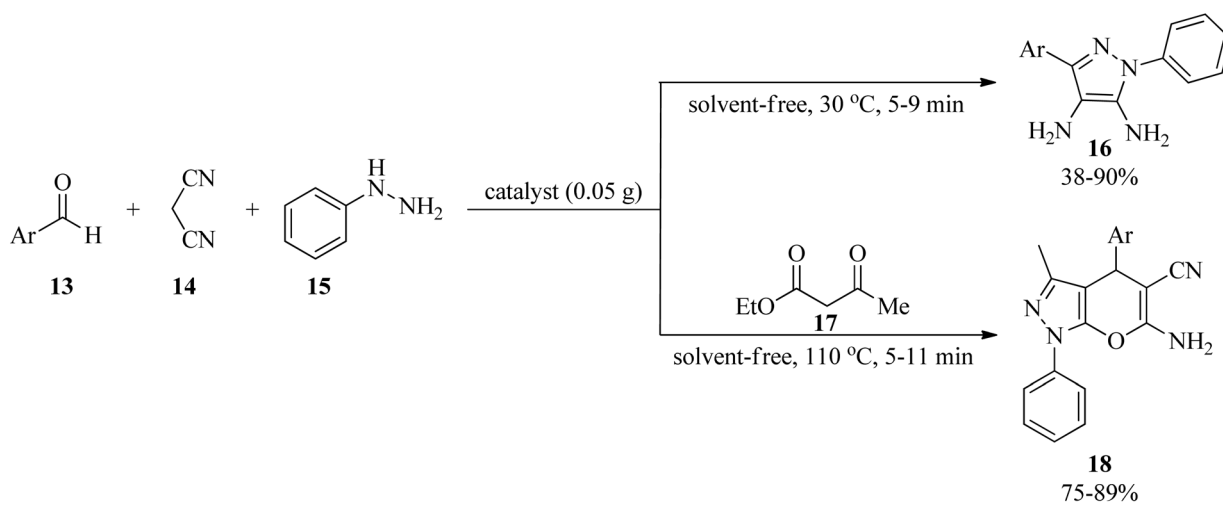


Scheme 4 Mechanism for the conversion of uracil to thymine.

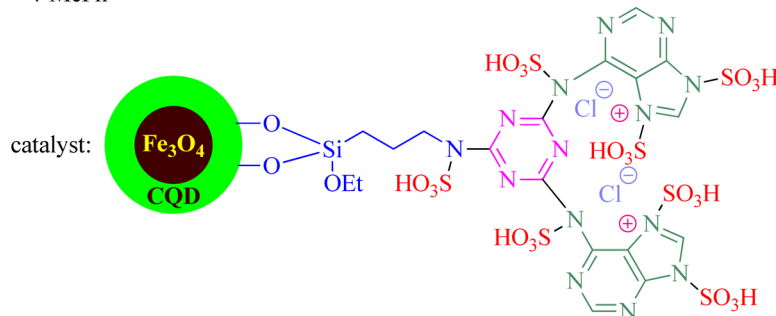
under different experimental conditions.<sup>28</sup> Barks *et al.* in 2010 reported the catalyst-free synthesis of adenine and guanine from UV-irradiated formamide solutions.<sup>29</sup> In addition, several mineral and metal oxide catalysts were utilized to obtain various DNA-nucleobases from formamide. Saladino *et al.* in 2001 reported the catalytic (in the presence of  $\text{CaCO}_3$ , silica, alumine, kaolin, and zeolite-Y) formation from neat formamide.<sup>30</sup> Some other catalytic systems to obtain DNA-nucleobases from the formamide substrate are:  $\text{TiO}_2$ ,<sup>31</sup> montmorillonites,<sup>32</sup> cosmic-dust analogues,<sup>33</sup> iron-sulfur and iron-copper-sulfur minerals,<sup>34</sup> zirconia,<sup>35</sup> common rock-forming minerals (such as silicates, and carbonates),<sup>36</sup> and iron oxides/hydroxides (hematite, goethite, and akaganeite).<sup>37</sup> In 2022, Nejdl *et al.* utilized ZnCd QDs upon UV irradiation in prebiotic liquid formamide to obtain some nucleobases with increased yields.<sup>38</sup> Oba *et al.* in 2019 achieved DNA-nucleobases (cytosine, uracil,

thymine, and adenine) in interstellar ice analogues composed of simple molecules, including  $\text{H}_2\text{O}$ ,  $\text{CO}$ ,  $\text{NH}_3$ , and  $\text{CH}_3\text{OH}$  after exposure to ultraviolet photons, followed by thermal processes.<sup>39</sup> In 2013, the preparation of adenine from formamide was considered a self-catalytic mechanism in an abiotic approach.<sup>40</sup>

A considerable number of enzymes consist of nucleobase motifs.<sup>41</sup> As some enzymes or enzyme complexes require several cofactors, they utilize nucleotide cofactors, including a purine base (usually adenine) binding site.<sup>42</sup> Adenine is an inextricable part of enzyme cofactors and second messenger systems, such as  $\text{NAD}^+$ ,  $\text{FADH}_2$ , and cAMP, which are essential for certain catalytic reactions and biochemical processes. In addition, a crucial catalytic role of the adenine moiety is also observed in group II intron catalysis and at the ribosomal peptidyl-transferase center.<sup>43</sup>

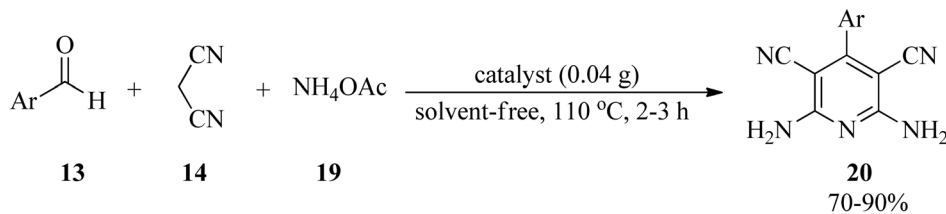


Ar = Ph, 4-FPh, 3-FPh, 4-ClPh, 2-ClPh, 2,4-(Cl)<sub>2</sub>Ph, 4-BrPh, 3-BrPh, 3-NO<sub>2</sub>Ph, 4-OHPh, 4-OMePh, 3,4-(OMe)<sub>2</sub>Ph, 4-MePh



Scheme 5 Synthesis procedure for 1H-pyrazole 4-carbonitrile and pyrano[2,3-c] pyrazoles.





Ar = Ph, 4-ClPh, 2-ClPh, 4-OHPh, 3-NO<sub>2</sub>Ph, 2-NO<sub>2</sub>Ph, 4-CHOPh, 3-OMePh, 5-OMe-6-OHPh, 3-OMe-4-OHPh, 2-furanyl

Scheme 6 Synthesis of 2,6-diamino-4-arylpyridine-3,5-dicarbonitriles.

Nucleobases and their derivatives reveal widespread biological and therapeutic activities in medicinal chemistry as notable pharmacophores,<sup>44,45</sup> antituberculosis agents,<sup>46</sup> kinase or cyclin-dependent kinase inhibitors,<sup>47,48</sup> antibiotics and biofilm inhibitors,<sup>49</sup> HIV viral capsid inhibitor,<sup>50</sup> antiviral (such as Human Immunodeficiency Virus and Hepatitis Virus),<sup>51-53</sup> antineoplastic agents,<sup>54</sup> and A3 adenosine receptor antagonists and ligands.<sup>55</sup>

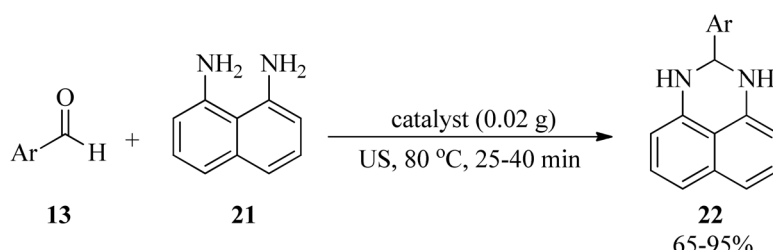
Nucleobases possess a wide range of applications in different branches of science and technology (with various roles such as organic/bio-catalyst, reagent, substrate, ligand, capping agent, and promoter) such as polymer preparation and/or modifications,<sup>56-58</sup> medicinal chemistry and therapeutic investigations,<sup>59</sup> *in vitro* and/or *in vivo* drug delivery<sup>60,61</sup> nanomaterials and nanotechnology,<sup>62-65</sup> electrochemistry and electrochemical sensors,<sup>66-70</sup> supramolecular chemistry,<sup>71-73</sup> metal-organic frameworks (MOFs) chemistry,<sup>74-76</sup> heterogeneous catalysts and/or catalytic systems,<sup>77-80</sup> batteries and energy-storage,<sup>81-83</sup> oxidation/reduction chemistry,<sup>84-87</sup> and biodiesel synthesis.<sup>88</sup> In 1999, some Cu(adenine)<sub>2</sub> complexes displayed the promotion of O<sub>2</sub> production from H<sub>2</sub>O<sub>2</sub> through the disproportionation of

hydrogen peroxide into oxygen and water.<sup>89</sup> Adenine-functionalized conjugated polymer PF6A-DBTO2 demonstrated high photocatalytic activity with hydrogen evolution from water.<sup>90</sup>

The plentiful resources of nucleobases and numerous interaction sites, for instance, hydrogen bonding,  $\pi$ - $\pi$  stacking, and van der Waals forces, enable them to interact and functionalize other molecules.<sup>91</sup> Based to these properties, the authors have reviewed the literature reports about the catalytic activity of nucleobases in various organic transformations. It must be mentioned that the number of reports for applications of adenine, cytosine, guanine, and thymine as a sole catalyst or part of the catalytic systems is few, so the catalytic role of each of the four DNA nucleobases is investigated in each part as below.

## 2. Catalytic activity of adenine in various organic transformations

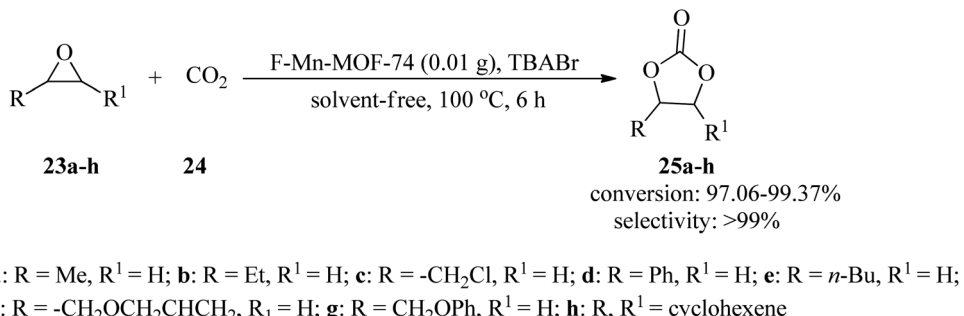
Owing to the key role of pyrazole motif in various fields of chemistry and biology,<sup>92-95</sup> Ahmadi *et al.* in 2023 presented a novel, applicable, and efficacious technique to prepare 5-



Ar = 4-OHPh, 3-NO<sub>2</sub>Ph, 2-NO<sub>2</sub>Ph, 3-OMePh, 2-OMePh, 3-MePh, 3,4-OMe<sub>2</sub>Ph, 2,5-Cl<sub>2</sub>Ph

Scheme 7 Preparation of 2,3-dihydro-2-aryl-1H-perimidines.

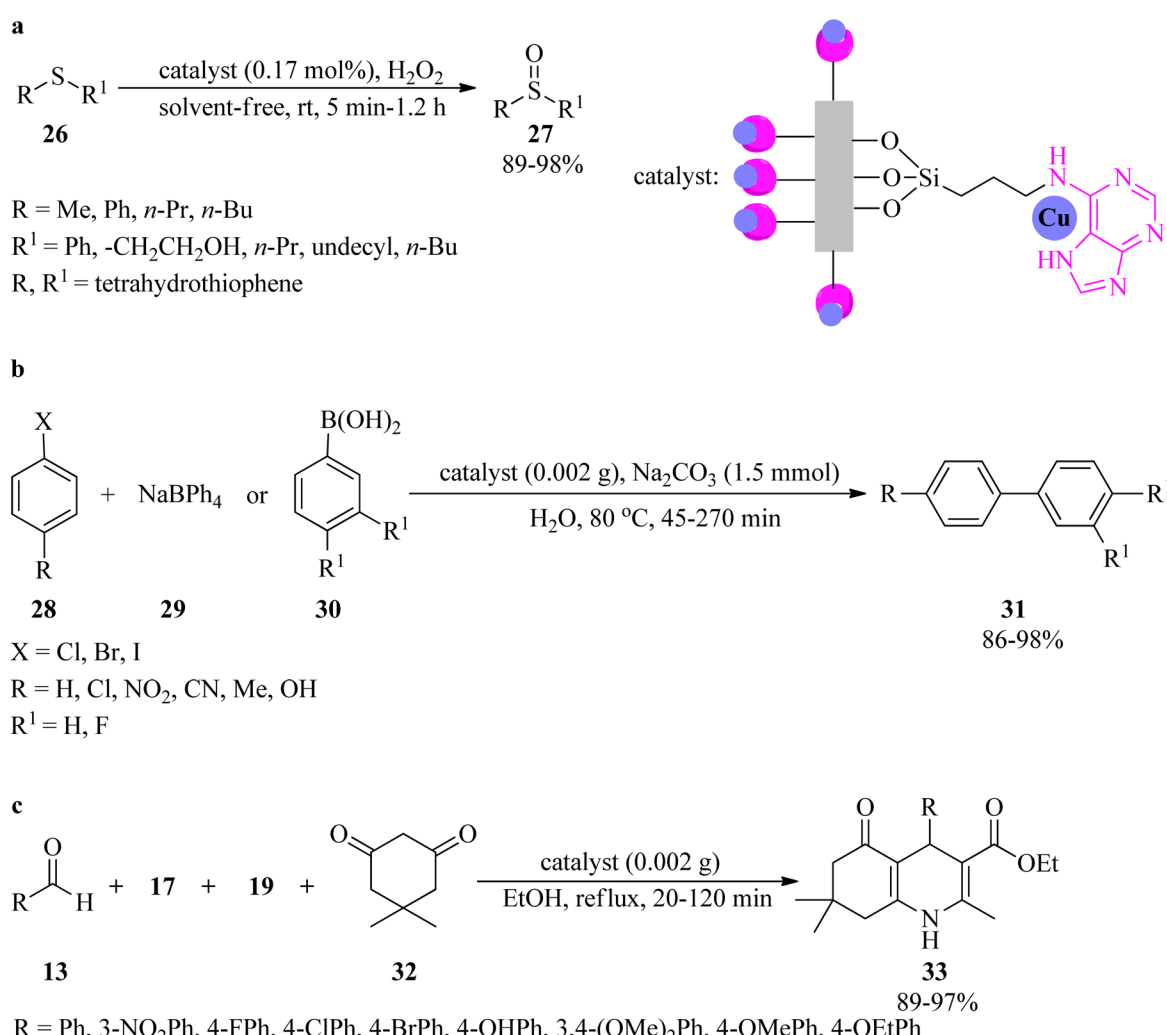




Scheme 8 Synthesis of cyclic unsymmetrical carbonates.

amino-1,3-diphenyl-1*H*-pyrazole 4-carbonitrile and pyrano[2,3-*c*]pyrazoles utilizing [Fe<sub>3</sub>O<sub>4</sub>@CQD@Si(OEt)(CH<sub>2</sub>)<sub>3</sub>-NH@CC@A@SO<sub>3</sub>H]<sup>+</sup>Cl<sup>-</sup> catalyst under solvent-free conditions. Firstly, the catalyst was synthesized *via* coating the Fe<sub>3</sub>O<sub>4</sub> magnetic nanoparticles with carbon quantum dots (CQD), followed by surface modification with (3-propylamine)-triethoxysilane, functionalization by cyanuric chloride (CC)

and adenine, and subsequent functionalization with chlorosulfonic acid. Then, 5-amino-1,3-diphenyl-1*H*-pyrazole 4-carbonitrile (**16**) was obtained *via* the condensation of equimolar amounts of aromatic aldehydes (**13**) with malononitrile (**14**) and phenyl hydrazine (**15**) at 30 °C in low to excellent yields (38–90%) and very short reaction times (5–9 min). On the other hand, the one-pot four-component condensation reaction of **13**,



Scheme 9 Various organic reactions in the presence of Cu-adenine@boehmite; (a) selective oxidation of sulfides to sulfoxides, (b) Suzuki coupling, and (c) synthesis of polyhydroquinolines.



**14**, **15**, and ethyl acetoacetate (**17**) realized pyrano[2,3-*c*]pyrazoles (**18**) within short reaction times in good yields (Scheme 5). The magnetic separability and recoverability of the catalyst were examined within 5 runs without notable activity loss.<sup>96</sup>

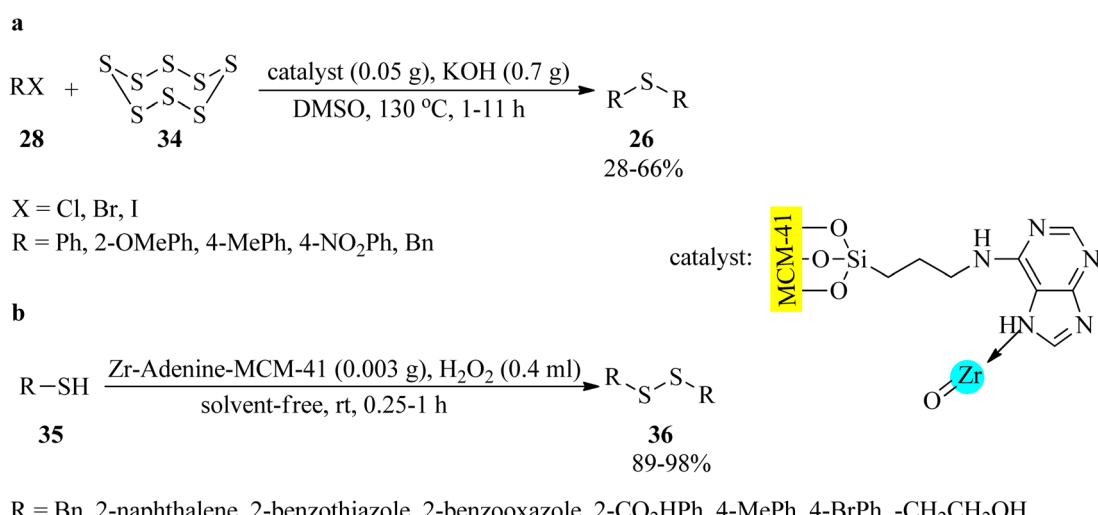
In 2022, Sadri *et al.* established a straightforward, convenient, and useful method for the production of 2,6-diamino-4-arylpyridine-3,5-dicarbonitrile (**20**) *via* the one-pot pseudo-four-component condensation reaction of aldehydes (**13**) with **14**, and ammonium acetate (**19**) utilizing a nanomagnetic catalyst coated with adenine and sulfonic acid ( $\text{Fe}_3\text{O}_4@-\text{SiO}_2@(\text{CH}_2)_3\text{NHCO}$ -adenine sulfonic acid), as a facile, cost-effective, recyclable, and reusable catalyst, under solvent-free conditions at 110 °C (Scheme 6). Mild reaction conditions, easy catalyst preparation, simple purification and isolation of the products (no chromatographical techniques) are some of the noteworthy features of this process.<sup>97</sup>

The same research group also subjected this catalyst for the synthesis of 2,3-dihydro-2-aryl-1*H*-perimidines (**22**) using aryl aldehydes (**13**) and 1,8-diamino naphthalene (**21**) under ultrasonic irradiation and solvent-free conditions (Scheme 7).<sup>98</sup> The recovery and reusability test of the nanostructure was successful within 4 runs.

In 2020, a highly effective, applicable, and green technique was presented for the formation of cyclic carbonates (**25a-h**) through the cycloaddition reaction of epoxides (**23a-h**) with carbon dioxide (**24**, 10 bar pressure) by flower-like manganesees confined metal-organic framework (F-Mn-MOF-74) as a catalyst and tetrabutylammonium bromide (TBABr) as a co-catalyst under solvent-free conditions at 100 °C within 6 h with excellent conversion and selectivity. In this research, in order to prepare F-Mn-MOF-74, adenine was applied as an alkali source and competitive ligand in comparison to the synthetic Mn-MOF-74. It was found that the spherical F-Mn-MOF-74 catalyst, along with TBABr, disclosed excellent catalytic performance in the cyclic esterification reaction. It should be noted that the catalytic system proceeded with the transformation of cyclohexene oxide with CO<sub>2</sub> (1 MP) at 160 °C within 24 h to

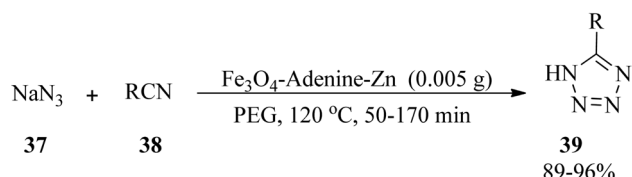
produce the corresponding cyclic carbonate in moderate conversion (51.98%) and excellent selectivity (92.65%) (Scheme 8).<sup>99</sup> Similarly, this transformation occurred at 80 °C in 8 h utilizing two new adenine-based Zn(II)/Cd(II)-MOFs, namely,  $[\text{Zn}_2(\text{H}_2\text{O})(\text{stdb})_2(5\text{H-A})(9\text{H-A})_2]_n$  (PNU-21) and  $[\text{Cd}_2(-\text{Hstdb})(\text{stdb})(8\text{H-A})(\text{A})]_n$  (PNU-22), including auxiliary dicarboxylate ligand (stdb = 4,4'-stilbenedicarboxylate). The catalysts were characterized through different techniques, such as single-crystal X-ray diffraction (SXRD), which disclosed 2D and 3D rigid and robust building blocks for PNU-21 and PNU-22, respectively, along with coordinately unsaturated metal surroundings. It should be mentioned that the presence of unsaturated Zn and Cd metals and basic N atoms in both catalysts converted them into acid-base efficient binary catalysts for the preparation of the corresponding products. The results demonstrated the better utility of PNU-21 (11–96%) in comparison to PNU-22 (8–85%).<sup>100</sup>

In 2023, a new adenine-functionalized dendritic fibrous nanosilica (DAD) was synthesized by functionalizing the surface of dendritic fibrous nanosilica (DFNS) with adenine using a bifunctional isocyanate crosslinker ((EtO)<sub>3</sub>Si(CH<sub>2</sub>)<sub>3</sub>NCO). This adenine-functionalized dendritic fibrous nanosilica was used as a bifunctional catalyst for CO<sub>2</sub> fixation in order to react with epoxide (**23**) to achieve cyclic carbonates (**25**). The reaction proceeded in the presence of TBAB (tetrabutylammonium bromide) co-catalyst under solvent-free conditions.<sup>101</sup> In 2005, the cycloaddition of CO<sub>2</sub> to epoxides (epichlorohydrin, propene oxide, and styrene oxide) to afford cyclic carbonates (**25**) occurred in the presence of adenine-modified Ti-SBA-15 catalysts. In addition, carbamates were synthesized through the reaction of alkyl/aryl amines, CO<sub>2</sub>, and *n*-butyl bromide. In the synthesis of cyclic carbonates, the reaction proceeded without any additional co-catalysts like *N,N*-dimethylaminopyridine (DMAP) or quaternary ammonium salts. The process using the present catalyst system avoids hazardous substances like phosgene or isocyanate and progresses at low temperatures and pressures.<sup>102</sup>

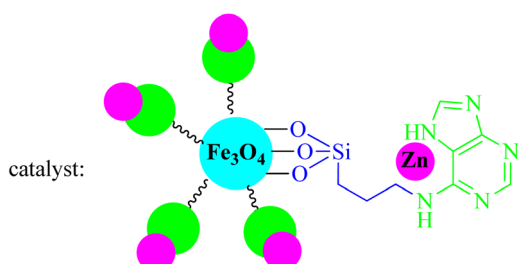


**Scheme 10** (a) Synthetic route to symmetrical sulfides, and (b) oxidative coupling reaction of thiols to disulfides in the presence of Zr-adenine-MCM-41.





R = Ph, 2-OHPh, 4-ClPh, 2-ClPh, 4-*i*-PrPh, 4-CNPh, 2-CNPh, 4-NO<sub>2</sub>Ph, 3-NO<sub>2</sub>Ph, 3-BrPh

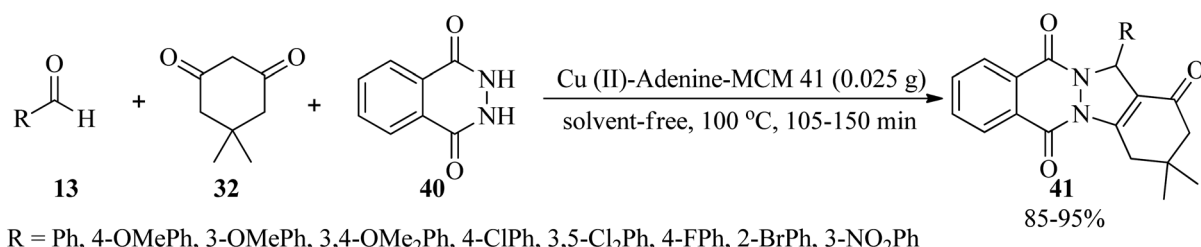


**Scheme 11** Synthesis of 5-substituted tetrazoles using sodium azide and benzonitriles.

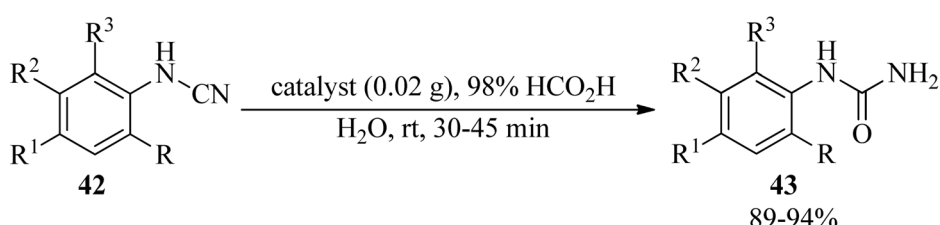
Rigid copper on adenine-coated boehmite nanoparticles ( $\text{Cu-adenine@boehmite}$ ) was prepared by Ghorbani-Choghamarani *et al.* in 2019, which catalyzed various organic transformations, such as the selective oxidation of sulfides (26) to sulfoxides (27) by hydrogen peroxide as an oxidant under solvent-free conditions at room temperature (Scheme 9a). On the basis of the

resulting data, diverse aromatic, aliphatic, and heterocyclic sulfides indicated no significant difference in the reaction yields, turnover numbers (TON), and turnover frequency (TOF) values. Generally, the aromatic sulfides prolong the reaction times. It is noteworthy that this transformation was not accompanied by forming sulfone as the by-product.<sup>103</sup> The adenine-containing catalyst also promoted the aqua-mediated formation of biphenyls (31) through the Suzuki C–C coupling reaction of aryl halides (28) with sodium tetraphenylborate (29) or phenylboronic acid derivatives (30) (in 1 : 0.5 and 1 : 1 molar ratios, respectively) utilizing sodium carbonate ( $\text{Na}_2\text{CO}_3$ ) as a base at 80 °C (Scheme 9b). Notably, the coupling of with aryl iodides was performed in shorter reaction times than other aryl halides (chloride and bromide). The selectivity of the catalyst was examined *via* the utilization of 1-bromo-4-chlorobenzene in the coupling reaction with phenylboronic acid and sodium tetraphenyl borate. The results affirmed that the chloro functional group remained intact and the Suzuki reaction occurred on the bromo functional group as the only product. The formation of polyhydroquinolines (33) in aqueous media *via* the four-component condensation reaction of benzaldehyde (13), ethyl acetoacetate (17), ammonium acetate (19), and dimedone (32) in a 1 : 1 : 1.3 : 1 molar ratio, utilizing Cu-adenine@boehmite, were also performed successfully (Scheme 9c).<sup>103</sup>

In 2018, Tamoradi *et al.* designed and characterized a zirconium complex of adenine coated on mesoporous silica MCM-41



**Scheme 12** Synthesis of 1*H*-indazolo[1,2-*b*]phthalazine-triones.



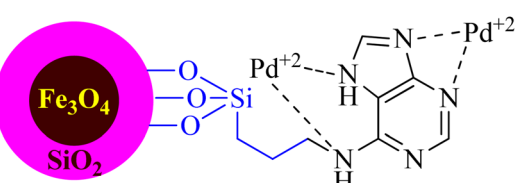
R = H, Cl

$R^1 = H, OMe, Me, Cl, Ac, NO_2$

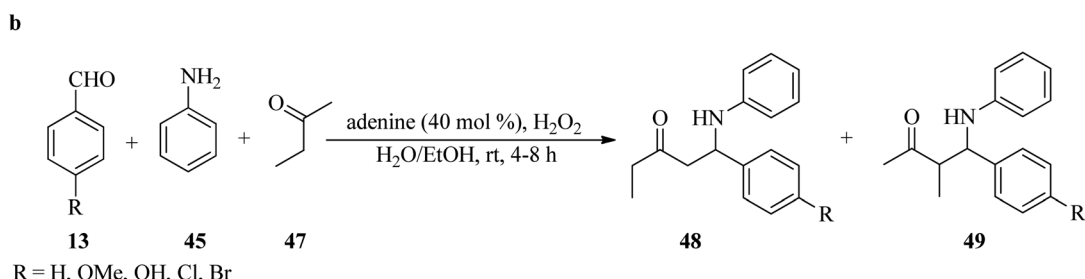
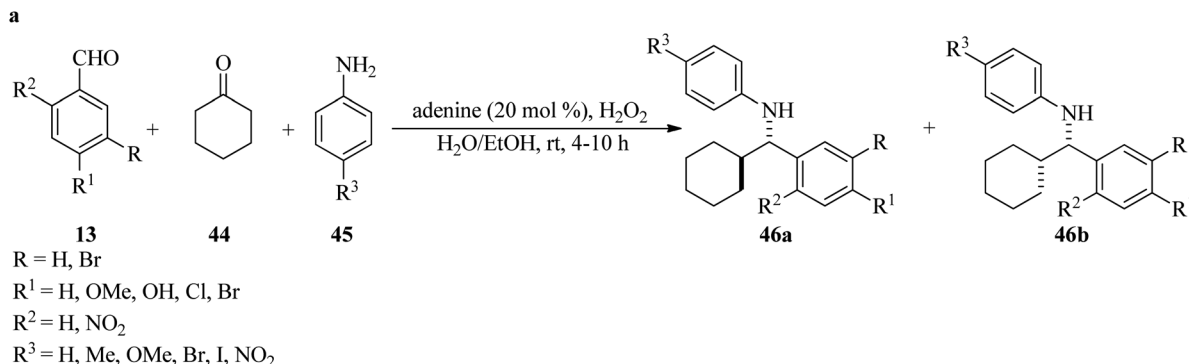
R<sup>2</sup> = H, Br, Cl

$R^3 = H, Me$

R<sup>2</sup> R<sup>3</sup> = Ph



**Scheme 13** Generation of *N*-mono-substituted ureas.

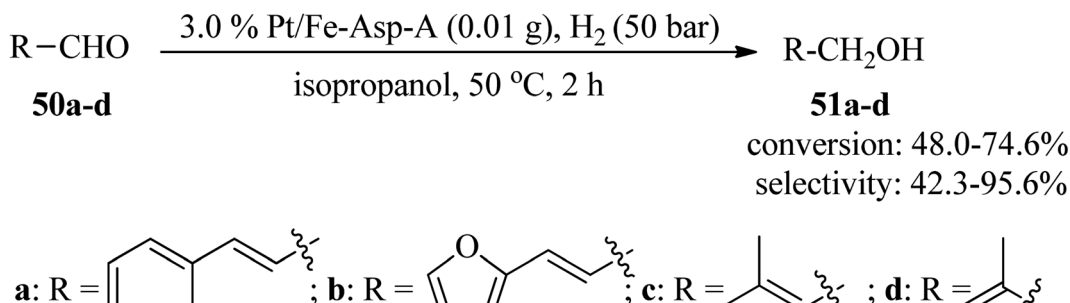


**Scheme 14** Adenine-mediated Mannich type reaction of (a) cyclohexanone, amines, and various benzaldehydes, and (b) 2-butanone, amines, and aldehydes.

(Zr-adenine-MCM-41) as a non-toxic and thermally stable nanocatalyst to accelerate the synthesis of symmetrical sulfides (26) *via* the dimethyl sulfoxide-mediated reaction of aryl halides (28) with sulfur (34) in equimolar amounts (Scheme 10a).<sup>104</sup> As illustrated in Scheme 10b, the oxidative coupling reaction of thiols (35) was also accomplished to afford disulfides (36) using catalytic amounts of Zr-adenine-MCM-41 by  $H_2O_2$  as the oxidative reagent under solvent-free conditions at room temperature in 89–98% yields and very short reaction times.<sup>104</sup> Solvent-less oxidation of diverse kinds of sulfides (26) to their corresponding sulfoxides (27) was also performed in the presence of MCM-41-adenine-Zr (0.004 g) at ambient temperatures using  $H_2O_2$  oxidant (0.4 mL) in short reaction times (5–65 min) and excellent yields (89–97%).<sup>104</sup> The recovery and the reusability test of Zr-adenine-MCM-41 demonstrated good results for the 3-run synthesis of sulfides and 6-cycles for the oxidation of sulfides and oxidative coupling of

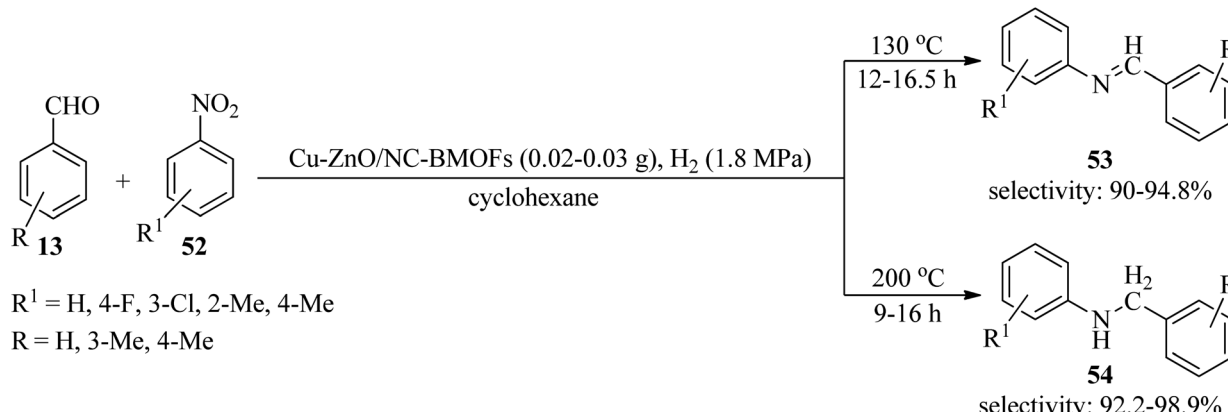
thiols. The observation described negligible leaching of zirconium from MCM-41-adenine-Zr.

Tamoradi *et al.*, in 2017, prepared a novel and green catalyst through the immobilization of Ni on magnetite nanoparticles coated with adenine ( $Fe_3O_4$ -adenine-Ni). The activity of the nanostructure was examined for the oxidation of sulfides (26) to sulfoxides (27) and oxidative coupling of thiols (35) to their corresponding disulfides (36) in the presence of  $H_2O_2$  oxidant (0.5 mL). The reactions were performed at ambient temperature under solvent-free conditions and ethanol media to achieve the desired products in short reaction times (12–70 min, 25–90 min) and excellent efficacy (94–98%, 87–97%).<sup>105</sup> The synthesis of polyhydroquinolines (33) *via* the refluxing ethanol-mediated four-component reaction of benzaldehydes (13), ethyl acetoacetate (17), ammonium acetate (19), and dimedone (32) in a 1 : 1 : 1.2 : 1 molar ratio, utilizing  $Fe_3O_4$ -adenine-Ni (0.05 g) was also performed successfully (145–255 min, 91–97%).<sup>105</sup>



**Scheme 15** Selective hydrogenation of cinnamaldehyde to cinnamyl alcohol.





Scheme 16 Synthesis of imines and secondary amines.

Zinc(II)-adenine complex functionalized on magnetite nanoparticles ( $Fe_3O_4$ -adenine-Zn) was synthesized and characterized in 2017. Its catalytic efficacy was tested for the synthesis of 5-substituted tetrazoles (39) *via* the reaction of sodium azide (37) with benzonitriles (38) in a 1.2:1 molar ratio (Scheme 11).<sup>106</sup>

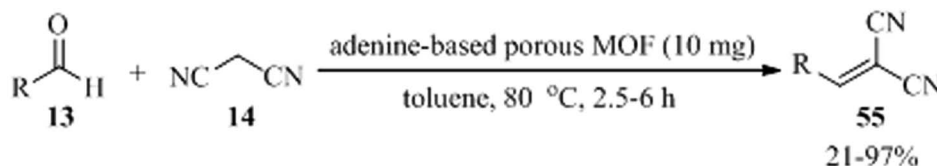
The catalyst was also utilized to promote the solvent-free oxidation of sulfides (26) to sulfoxides (27) using  $H_2O_2$  oxidant in 15–130 min with excellent yields (89–98%). The oxidative coupling of thiols (35) to their corresponding disulfides (36) also occurred in the presence of  $Fe_3O_4$ -adenine-Zn in ethyl acetate media at room temperature within 40–130 min by 86–99%.<sup>106</sup> A wide range of thiols (aliphatic, aromatic, and heterocyclic) were successfully subjected to the mentioned oxidative reactions. This catalyst could be recovered easily and reused at least six times without significant loss of its catalytic activity.

5-Substituted 1*H*-tetrazoles (39) were also obtained through the reaction of sodium azide (37) and benzonitrile (38) in a 1.2:1 molar ratio in the presence of a Cu(II) complex supported in MCM-41 channels modified with adenine (Cu(II)-adenine-MCM-41 catalyst, 35 mg) in PEG-400 at 130 °C in 3–20 min and 70–92% yield.<sup>107</sup> 1*H*-indazolo[1,2-*b*]phthalazine-triones (41) were also obtained through the solvent-free reaction of various benzaldehydes (13), dimedone (32), and phthalhydrazide (40) in a 1:1.2:1 molar ratio at 100 °C (Scheme 12).<sup>107</sup> The catalyst is a Cu(II)-Schiff-base complex supported on MCM-41, which was successfully prepared *via* the post-grafting method.

In 2023, Khorram Abadi *et al.* examined the hydrolysis of cyanamides (42) by formic acid in water media in the presence of palladium(II)-adenine complex coated on the surface of

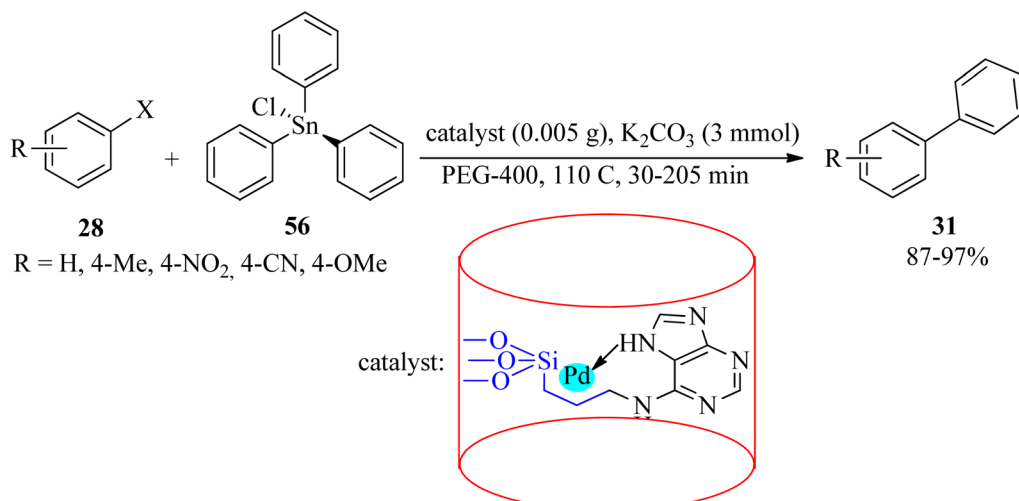
a silica-modified magnetic catalyst by employing 3-chloropropyltrimethoxysilane (CPTMS) as a linker and ( $Fe_3O_4$ @SiO<sub>2</sub>@CPTMS@A@Pd), as a new, efficient, and recyclable heterogeneous nanocatalyst at room temperature to obtain *N*-mono-substituted ureas (43) in high yields and short reaction times (Scheme 13). The catalytic system progressed well with all kinds of aryl cyanamides containing electron-donating and electron-withdrawing substituents.<sup>108</sup> The catalyst was effective for five consecutive runs. The role of formic acid is probably to protonate the –CN group to increase its polarity. Also, it could protonate water to give  $H_3O^+$  and  $HCOO^-$  to assist Pd in hydrolyzing CN to  $CONH_2$ .

In 2009, Goswami and Das developed an environmentally friendly approach for the diastereoselective synthesis of Mannich base products (46) *via* a three-component Mannich-type reaction of benzaldehydes (13), cyclohexanone (44), and anilines (45), utilizing adenine as an aminocatalyst (20 mol%) and  $H_2O_2$  (30%, 4  $\mu$ L) as additive in a mixture of water and ethanol (1/4) media at room temperature in 4–10 h in good to excellent yields (80–95%). It is significant that anilines, with electron-donating groups, resulted in the major generation of *anti*-products (46a) while the electron-withdrawing substituents (such as nitro and iodo) attained *syn*-form (46b) as the main products (Scheme 14a).<sup>109</sup> It is necessary to mention that the condensation of cyclohexanone (47) and aniline, with both electron-donating and electron-withdrawing benzaldehydes, occurred successfully in high to excellent yields (75–93%). The stereochemical outcome appears to be unaffected, with the anti-isomer being the main product. Remarkably, the reaction with aliphatic aldehydes was unsuccessful. Replacing cyclohexanone



Scheme 17 Knoevenagel condensation of malononitrile with different aldehydes.



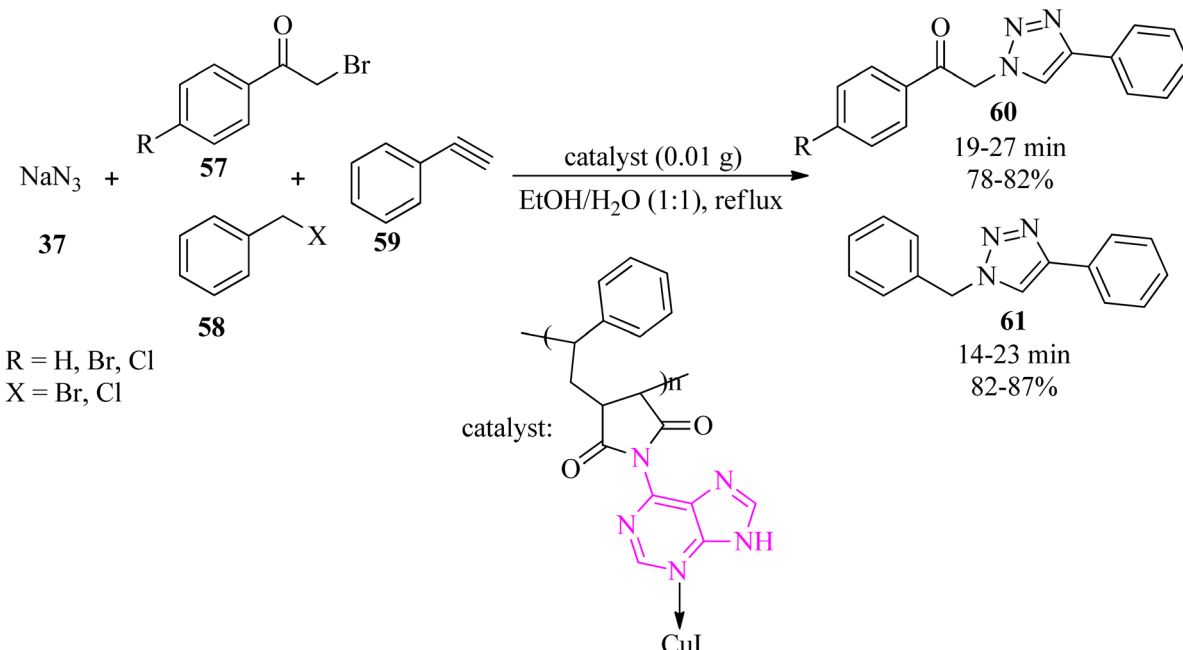


Scheme 18 Stille cross-coupling reaction of aryl halides with triphenyltin chloride.

with 2-butanone (**47**), as an unsymmetrical acyclic ketone, yielded two regiosomers **48** and **49**, in which product **49** produced a mixture of diastereomers where the *anti*-diastereomers were the major products (Scheme 14b).<sup>109</sup> In this transformation, the reactivity of 4-butanone was lower than that of cyclohexanone and 40 mol% of organocatalyst was needed for completion. The absence of column chromatography for majority of the compounds partially overcomes the major problem of epimerization of the Mannich products.<sup>110</sup>

In 2020, the rigid palladium-adenine complex on modified boehmite nanoparticles (Pd-adenine@boehmite) was introduced as a beneficial, recoverable, and reusable heterogeneous nanocatalyst for the aqua-mediated preparation of biphenyls (**31**) through the Suzuki coupling reaction of aryl halides (**28**)

with sodium tetraphenylborate (**29**) or phenylboronic acid derivatives (**30**) utilizing sodium carbonate (Na<sub>2</sub>CO<sub>3</sub>) as the base at 80 °C within 0.5–4 h in high to excellent yields (85–96%).<sup>111</sup> Notably, the resulting TOF values for aryl halides affirmed their reactivity as PhI > PhBr > PhCl. Furthermore, aryl halides bearing an electron-withdrawing group were more reactive. Sodium tetraphenylborate or phenylboronic acid derivatives have no significant influence on the yields. In addition, the [3 + 2] cycloaddition reaction of sodium azide (**37**) with benzonitriles (**38**) in PEG at 120 °C using Pd-adenine@boehmite resulted in 5-substituted tetrazoles (**39**) in 0.3–21 h and good to excellent yields (85–96%). Both electron-donating and electron-withdrawing benzonitriles resulted in products with good yields and appropriate TOF numbers.<sup>111</sup>



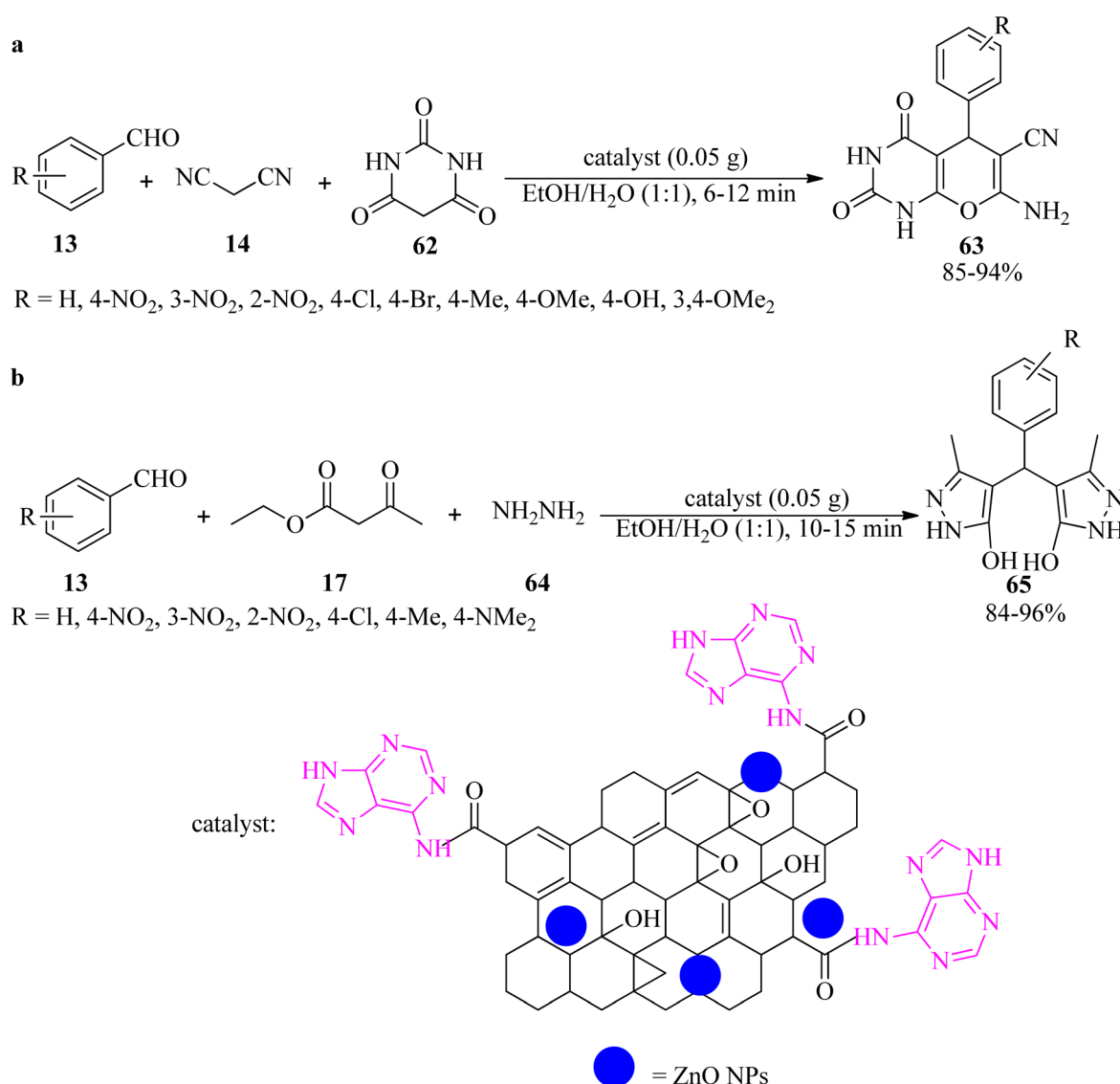
Scheme 19 Synthesis of 1,4-disubstituted 1,2,3-triazoles via click reaction.



Cinnamyl alcohol is a significant chemical intermediate utilized in medicines, flavorings, and food additives. Cinnamyl alcohol is mainly produced through the selective hydrogenation of cinnamaldehyde.<sup>112-114</sup> Hence, Tang *et al.*, in 2022, employed an amorphous Pt/Fe-Asp-A nanocatalyst for chemoselective hydrogenation of cinnamaldehydes. Adenine was utilized as a reinforcing agent to improve the chemical stability and selectivity of the Fe-L-aspartic (Fe-Asp) coordination material, which was modified through the loading of platinum nanoparticles on its surface. Finally, the resultant amorphous 3.0% Pt/Fe-Asp-A nanocatalyst catalyzed the reaction of cinnamaldehyde (**50a**) with hydrogen ( $H_2$ ) at 20 bar in the presence of isopropanol at 50 °C to furnish cinnamyl alcohol (**51a**) in a 2 h period with excellent selectivity (91.2%) and conversion (93.1%). The amorphous 3.0% Pt/Fe-Asp-A nanocatalyst also exhibited good performance to promote various  $\alpha,\beta$ -unsaturated aldehydes (**50a-d**) under similar conditions with 48.0-

74.6% conversion and 42.3–95.6% selectivity (Scheme 15). The recyclability and reusability of the synthesized nanocatalyst have been successfully investigated in up to ten runs without any considerable loss in catalytic activity.<sup>115</sup>

In 2021, a bimetallic CuZn-MOFs was generated *via* a facile solvothermal method utilizing adenine biomolecule as an organic linker. Moreover, a ZnO/nitrogen-doped carbon composite immobilized Cu catalyst (Cu-ZnO/NC-BMOFs) from CuZn-MOFs was obtained through a one-pot pyrolysis procedure. Then, its catalytic activity was examined by the hydrogenation/amination tandem reaction of benzaldehydes (13) and substituted nitroarenes (52) in cyclohexane *via* two pathways: (a) production of imines (53) at 130 °C in 12–16.5 h with high selectivity (90–94.8%), (b) generation of secondary amines (54) at 200 °C with high activity and high selectivity (92.2–98.9%) (Scheme 16). Comparatively, the Cu/ZnO/NC-IWI catalyst, prepared by incipient wetness impregnation,



**Scheme 20** Synthesis of (a) pyrano[2,3-*d*]pyrimidines, and (b) bis(pyrazol-5-ole) derivatives

promoted the hydrogenation/amination reaction of nitrobenzene with benzaldehyde to give *N*-benzylaniline as compared to the CuZn-MOFs, and the conversion of nitrobenzene and selectivity toward *N*-benzylaniline was lower (49.6% and 10.9%). High selectivities, good stability, recyclability, and reusability of the catalyst are some of the advantages of this method.<sup>116</sup>

A novel adenine-based porous MOF, named  $[H_2N(CH_3)_2] \cdot [Zn_4(L)_{1.5}(ad)_3(H_2O)_2] \cdot 4DMF$  (denoted as JUC-188, DMF = *N,N*-dimethylformamide), was prepared utilizing tetracarboxylic acid organic ligand, namely 5,5'-(1,3,6,8-tetraoxobenzo[Imn][3,8]phenanthroline-2,7-diy)bis-1,3-benzenedicarboxylic acid ( $H_4L$ ), and adenine (ad) as organic linker.  $H_4L$  and ad are both successfully connected to Zn(II) ions. There are three different inorganic clusters in JUC-188, including  $ZnO_2N_2$ ,  $Zn_2O_2N_6$ , and  $ZnO_5N$  clusters. The Knoevenagel condensation of different aldehydes (**13**) and malononitrile (**14**), in a 1 : 1.1 molar ratio, in the presence of JUC-188 as a solid catalyst has been examined successfully (Scheme 17).<sup>117</sup> In the case of small aldehydes, the results are satisfactory. But for 1-naphthaldehyde and 9-anthracenecarboxaldehyde, the yields are very low, even with prolonged reaction times of 6 h with 43% and 21% yields, respectively. So, the catalyst is referred to as size-selective. Furthermore, it showed that adenine ligands can be applied to construct MOFs with the Lewis basic sites ( $-NH_2$ ) as heterogeneous catalysts.

In 2019, palladium anchored on the surface of adenine-modified mesoporous silica was used to obtain SBA-15@adenine-Pd. Its efficacy was examined in the Stille cross-coupling reaction of different aryl halides (**28**) with triphenyltin chloride (**56**) with a 1 : 0.5 molar ratio in PEG-400 media at 110 °C (Scheme 18).<sup>118</sup>

The mesoporous silica-anchored SBA-15@adenine-Pd also promoted the Suzuki coupling of equimolar amounts of various aryl halides (**28**) with phenylboronic acid (**30**) in hot (110 °C) PEG-400 media in the presence of  $K_2CO_3$  to obtain the corresponding biphenyl adducts (**31**) in 30–160 min and 83–98% yield.<sup>118</sup> SBA-15@adenine-Pd was also effective for the synthesis of symmetrical sulfides (**27**) via the reaction of aryl halides (**28**) and sulfur (**34**) in DMSO at 130 °C in the presence of KOH (0.5 g) to afford the desired products within 80–610 min by 43–79%.<sup>118</sup> The prepared catalyst separation could be easily achieved through filtration and drying after each run and can be reused

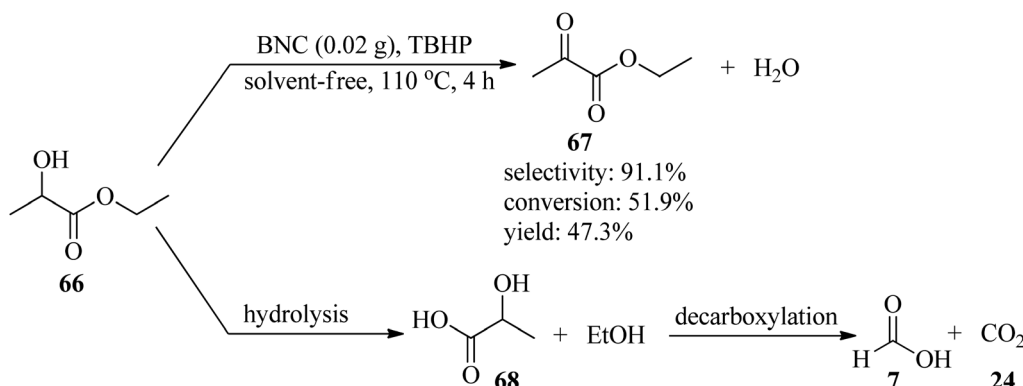
for several consecutive cycles without a considerable decrease in its catalytic activity in all three types of the mentioned reactions.

Novel adenine-based nano Cu(I) polymers were obtained via the immobilization of Cu(I) nanoparticles on modified poly(styrene-*co*-maleic anhydride) by adenine (Af-SMA-CuI). Its efficacy was successfully examined in the regioselective synthesis of 1,4-disubstituted 1,2,3-triazoles (**60**)/(**61**) via the click reaction of sodium azide (**37**),  $\alpha$ -haloketones (**57**)/alkyl halide (**58**), and alkyne (**59**), in a 1.2 : 1:1 molar ratio, to give the corresponding products (**60**)/(**61**) in satisfactory yields (78–87%). The copper content in the catalyst was determined to be 23.83% (w/w), and each gram of the heterogeneous catalyst includes 1.25 mmol of copper (Scheme 19).<sup>119</sup>

In 2020, the adenine-grafted carbon-modified amorphous ZnO nanocatalyst (ZnO@AC) was derived from garment industry waste (waste cotton cloth). It promoted the synthesis of pyrano[2,3-*d*]pyrimidines (**63**) via the reaction of aldehydes (**13**), malononitrile (**14**), and barbituric acid (**62**) in EtOH/H<sub>2</sub>O at ambient temperature (Scheme 20a).<sup>120</sup> The catalyst is also effective for the domino-type synthesis of bis(pyrazol-5-ole) derivatives (**65**) via the pseudo-five-component reaction of aromatic aldehydes (**13**), ethyl acetoacetate (**17**), and hydrazine hydrate (**64**), in a 1 : 2 : 2 molar ratio, at room temperature (Scheme 20b). The photocatalytic evaluation of ZnO@AC was performed on the methyl orange (MO) dye under UV light, with 87.3% degradation efficiency in 75 min. Moreover, the catalyst was recyclable and could be reused for up to eight runs, making it more sustainable.<sup>120</sup>

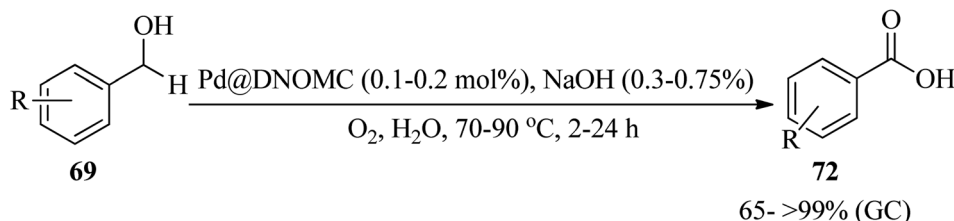
### 3. Catalytic activity of guanine in two- and multi-component reactions

In 2012, a cost-effective, metal-free, and template-free methodology was presented for the generation of boron (B) and nitrogen (N) co-doped carbon nanosheets (BNC), utilizing biomolecule guanine as the carbon (C) and N sources and boric acid as the B precursor. In the obtained BNC, guanine forms the G-quartet unit cells and expands to a larger planar network structure through multiple hydrogen bonds as both C and N sources. Subsequently, the resultant BNC catalyzed a liquid phase selective oxidation of ethyl lactate (EL, **66**) to ethyl

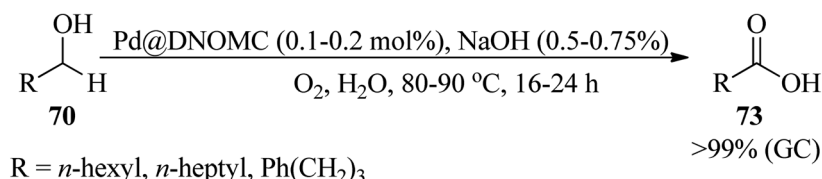


Scheme 21 Preparation of ethyl pyruvate (EP) from ethyl lactate (EL).

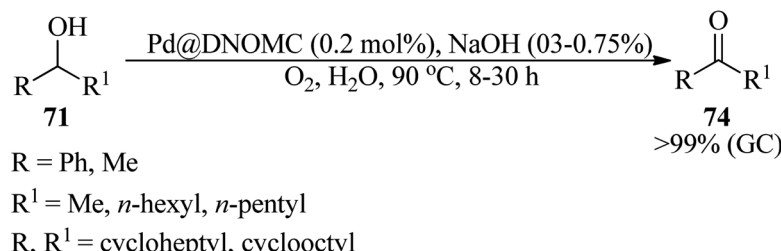




R = H, 4-Me, 3-Me, 2-Me, 4-OMe, 3-OMe, 2-OMe, 4-Cl, 3-Cl, 2-Cl, 4-*i*-Pr



R = *n*-hexyl, *n*-heptyl, Ph(CH<sub>2</sub>)<sub>3</sub>



R = Ph, Me

R<sup>1</sup> = Me, *n*-hexyl, *n*-pentyl

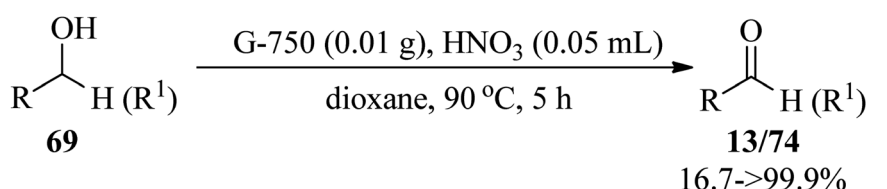
R, R<sup>1</sup> = cycloheptyl, cyclooctyl

Scheme 22 Aerobic alcohol oxidation using Pd@DNOMC.

pyruvate (EP, 67) by *tert*-butyl hydroperoxide (TBHP) as an oxidant under solvent-free conditions at 110 °C for 4 h with excellent selectivity (91.1%) and moderate conversion (51.9%) and yield (47.3%). This transformation was accompanied by the production of ethanol and lactic acid (68) as by-products through hydrolysis, which could be attributed to the instability of the ester functional group at elevated temperatures. Then, decarboxylation of the resulting lactic acid yielded formic acid (7) and CO<sub>2</sub> (24) (Scheme 21). On the other hand, the selective reduction of nitrobenzene (52) in the presence of hydrazine hydrate (64) under solvent-free conditions at 100 °C within 4 h afforded aniline (45) with excellent selectivity (95.5%), conversion (97.9%), and yield (93.5%). It is worth noting that in order to affirm the usefulness of the protocol, the oxidation and reduction reactions were carried out under

catalyst-free conditions and in the presence of different catalysts such as graphene, nitrogen-doped carbon (NC), oxidized carbon nanotubes (oCNT), BNC-1 and BNC-2 (containing lower boric acid, and lower amounts of B, N and O), and according to the resulting data, the utilization of BNC was more efficient.<sup>121</sup> The authors claimed that the guanine biomolecule leads to the formation of a graphitic structure during carbonization.

In 2022, Alizadeh *et al.* reported for the first time the synthesis of DES-derived nitrogen-rich ordered mesoporous carbon (DNOMC) with a three-dimensional cubic framework utilizing highly ordered mesoporous silica KIT-6 (arising from pluronic P123, *n*-butanol, and (EtO)<sub>4</sub>Si) and a deep eutectic solvent (DES) bearing choline chloride and D-glucose as starting materials. The reaction progressed *via* the addition of guanine and urea as nitrogen sources to the resultant DES and

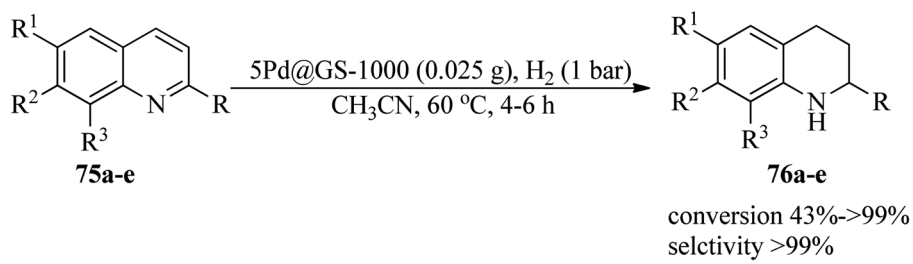


R = Ph, 4-MePh, 4-OMePh, 4-BrPh, 2-NO<sub>2</sub>Ph, biphenyl, 2-naphthyl

R<sup>1</sup> = H, Me, Ph

Scheme 23 Selective oxidation of benzyl alcohols.





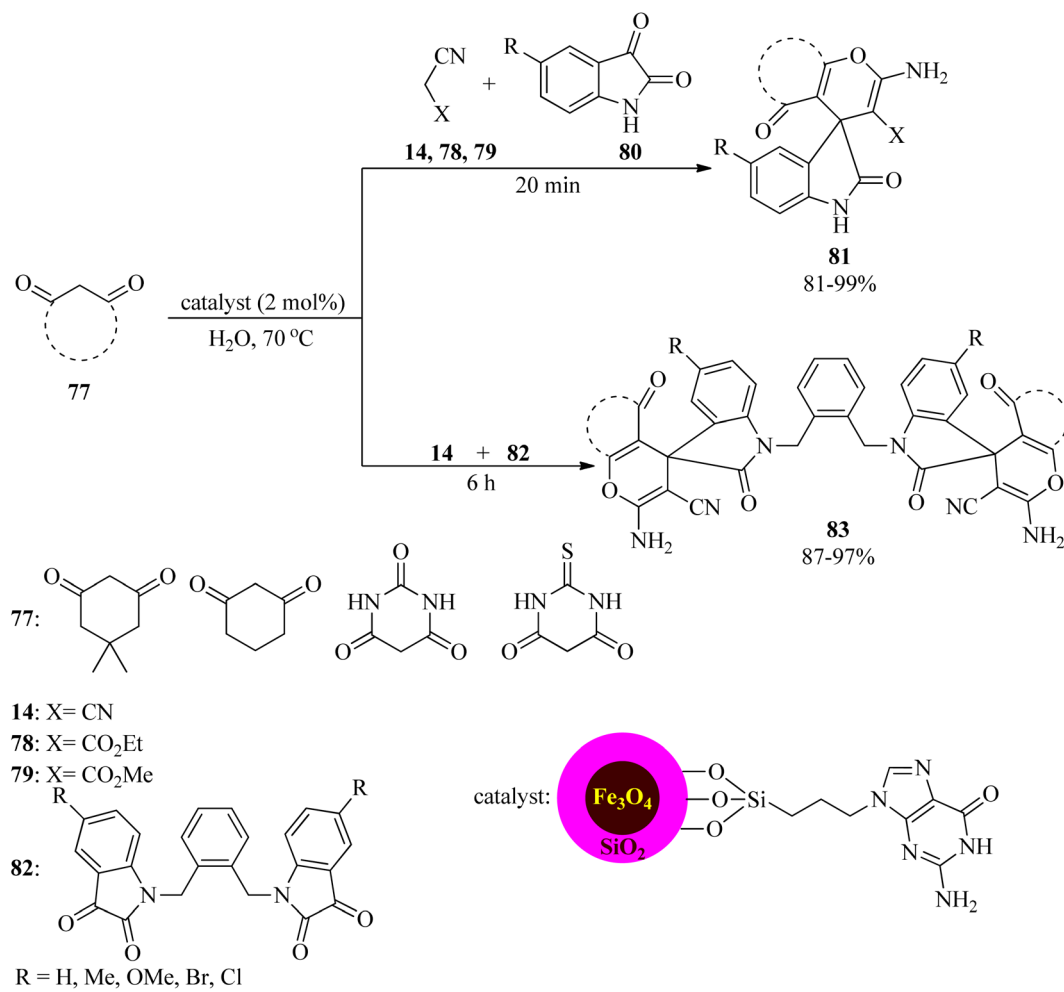
**a:** R, R<sup>1</sup>, R<sup>2</sup>, R<sup>3</sup> = H; **b:** R = Me, R<sup>1</sup>, R<sup>2</sup>, R<sup>3</sup> = H; **c:** R, R<sup>2</sup>, R<sup>3</sup> = H, R<sup>1</sup> = Me;  
**d:** R, R<sup>1</sup>, R<sup>3</sup> = H, R<sup>2</sup> = Me; **e:** R, R<sup>1</sup>, R<sup>2</sup> = H, R<sup>3</sup> = Me

Scheme 24 Hydrogenation of quinolones.

subsequent carbonization by the KIT-6 template. The resulting DNOMC was employed as a powerful and efficacious support for the stabilization of palladium nanoparticles (Pd@DNOMC). Subsequently, the catalytic system proceeded *via* the aqua-mediated aerobic oxidation of diverse primary and secondary benzylic alcohols (**69**) as well as cyclic and acyclic aliphatic alcohols (**70/71**) to the corresponding carboxylic acids (**72/73**) (in 65 → 99% yields) and ketones (**74**) (>99% yields) within 2–30 h at 70 °C by NaOH in the presence of molecular oxygen

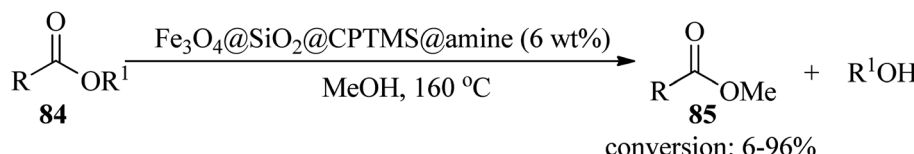
(Scheme 22). High yields, low cost, easily available substrates, experimental accessibility, recoverability, and reusability of the catalyst for up to ten runs without any considerable loss of efficiency are some of the advantages of this strategy. In this research, the hot filtration test showed that the catalyst works through a boomerang-type catalyst route.<sup>122</sup>

In 2023, Li *et al.* expressed a simple and metal-free procedure to synthesize *in situ* nitrogen-doped nanosheets through the pyrolysis of guanine at 750 °C, in which the guanine was chosen



Scheme 25 Preparation of 2',5-dioxo-5,6,7,8-tetrahydrospiro[chromene-4,3'-indoline]-3-carbonitriles and substituted dihydro-2-oxopyrroles.





84: soybean oil

85: biodiesel

amine= guanine, piperazine, methylamine, morpholine, aniline, melamine, ethylenediamine, (3-aminopropyl)triethoxysilane

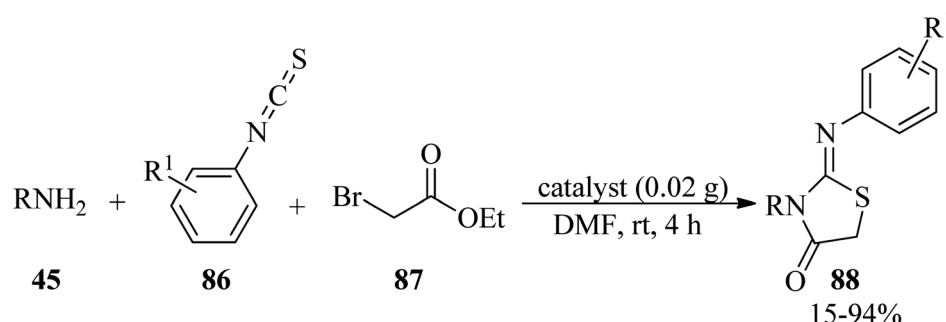
Scheme 26 Biodiesel production from soybean oil.

as the C and N precursor. The resulting N-doped nanocarbons (G-750) displayed a two-dimensional (2D) structure and high surface areas, which gave rise to excellent catalytic performance in the selective oxidation of benzyl alcohols (69) into benzaldehydes (13) or ketones (74) in 16.7%–99.9% yields by nitric acid as oxidant in 1,4-dioxane at 90 °C within 5 h (Scheme 23). It must be mentioned that graphitic nitrogen, pyridine nitrogen, and hydroxyl on the surface of nanocarbons play a key role in the reaction, in which the transformation of benzyl alcohol into benzaldehyde is mostly attributed to the concentration of hydroxyl groups, whereas the ratio of graphitic nitrogen and pyridine nitrogen has an important influence on the selectivity of benzaldehyde. Hence, the reactivity of benzyl alcohols bearing electron-donating groups was better than the alcohols with electron-withdrawing substituents, which could be ascribed to the inactivation of hydroxyl groups in catalytic reactions by the electron-withdrawing group.<sup>123</sup>

In 2019, Ng *et al.* prepared a novel palladium-guanine-reduced graphene oxide nanocomposite (Pd/rGO<sub>G</sub>) *via* an easy, scalable, one-pot microwave-assisted method, which

introduced guanine to the reduced graphene oxide-supported palladium *via* non-covalent functionalization. The abundant amino, amide, and imino functional groups of guanine are considered to be the anchoring sites, which allow the uniform distribution of palladium nanoparticles (of various shapes, such as triangular, rectangular, circular, and diamond). The Pd/rGOG is an efficient catalyst for methanol oxidation. In addition, the guanine is revealed to be catalytically active toward the methanol oxidation reaction, serving as a second catalyst.<sup>124</sup>

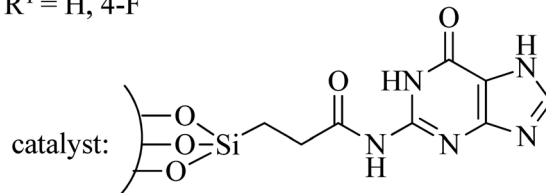
Hu *et al.* successfully designed a sustainable strategy for the synthesis of highly active and stable catalysts of N-doped and N/S-doped carbon nanosheet-coated palladium nanoparticles utilizing guanine or guanine sulfate as the nitrogen and carbon precursor, named Pd@G-1000 and Pd@GS-1000, respectively. The catalytic application was examined in the hydrogenation reaction of quinolones (75) under H<sub>2</sub> (1 bar) in CH<sub>3</sub>CN solvent at 60 °C (Scheme 24). The 5Pd@GS1000 catalyst indicated considerably improved activity with >99% conversion for 1,2,3,4-tetrahydroquinoline (76a) in comparison with 5Pd@G-1000 with 63% conversion.<sup>125</sup>



R = *n*-Pr, NH<sub>2</sub>(CH<sub>2</sub>)<sub>2</sub>, Ph, Bn, 4-ClBn, 2-ClBn, 3-OMeBn, 3-BrBn,

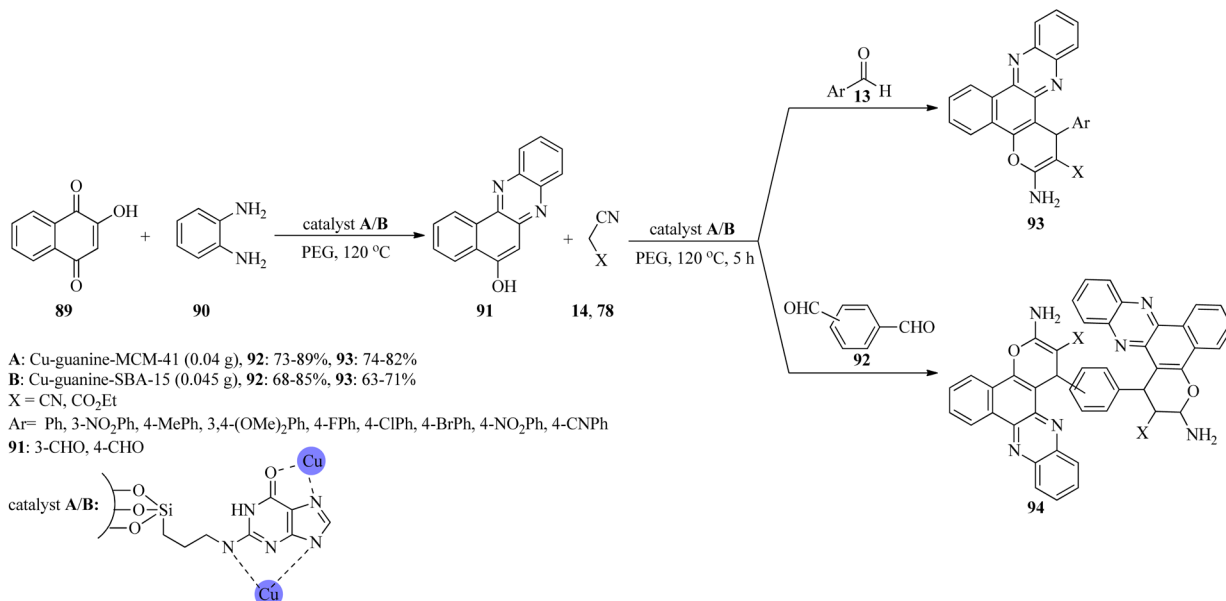
4-MeBn, 4-OMeBn, 4-FBn, 2-methylenefuryl

R' = H, 4-F



Scheme 27 Synthesis of 2-iminothiazolidin-4-ones.



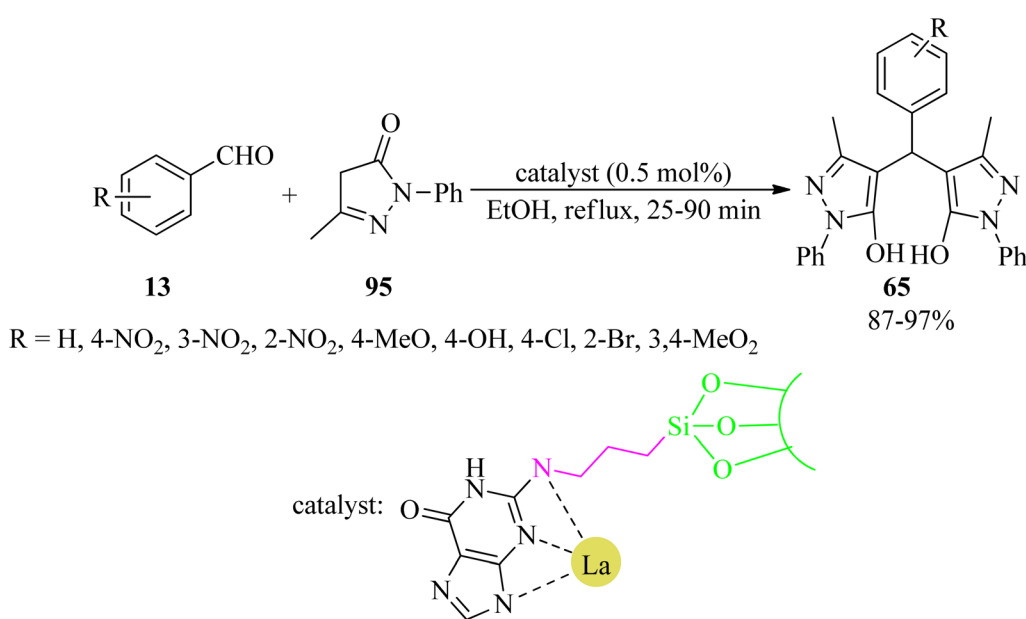


Scheme 28 Generation of benzo[c]pyrano[3,2-a]phenazines and bis-benzo[c]pyrano[3,2-a]phenazines.

In 2021, Saberi *et al.* prepared and characterized a novel nanocomposite *via* guanine embedded on the surface of a silica-modified magnetic catalyst, using 3-chloropropyltrimethoxysilane (CPTMS) as a linker ( $\text{Fe}_3\text{O}_4@\text{SiO}_2@\text{CPTMS}@$ guanine) and then its catalytic activity was investigated for the preparation of 2',5-dioxo-5,6,7,8-tetrahydrospiro[chromene-4,3'-indoline]-3-carbonitriles (81) through the one-pot three-component reaction of equimolar amounts of 1,3-dicarbonyls (77), reactive methylene derivatives (14, 78, 79), and isatins (80) in aqueous media at 70 °C in 81–99% for 20 min. The magnetite nanoparticles (2 mol%) also catalyzed the aqua-mediated

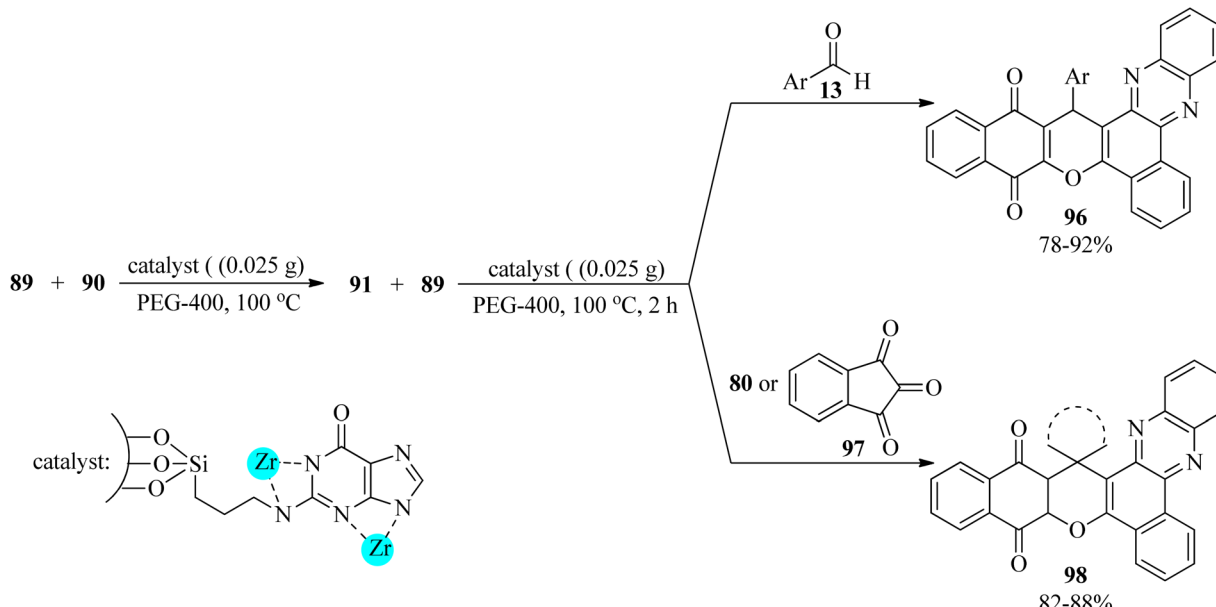
synthesis of substituted dihydro-2-oxopyrroles (83) by the one-pot multi-component reaction of 14, 1,3-dicarbonyls (77), and bis(isatin) derivatives (82), in a 2:2:1 molar ratio, at 70 °C (Scheme 25). Mild reaction conditions, easy separation of the catalyst from the reaction mixture by an external magnet, recyclability and reusability of  $\text{Fe}_3\text{O}_4@\text{SiO}_2@\text{CPTMS}@$ guanine to promote the reaction for ten runs without any appreciable loss of efficiency, easy work-up, and excellent yields are some of the advantages of this procedure.<sup>126</sup>

In 2018, Farzaneh *et al.* produced several  $\text{Fe}_3\text{O}_4@\text{SiO}_2@\text{CPTMS}@$ amine nanocomposites utilizing various amines, such



Scheme 29 Synthesis of 4,4'-(arylmethylene)-bis-(3-methyl-1-phenyl-1H-pyrazol-5-ol) derivatives.

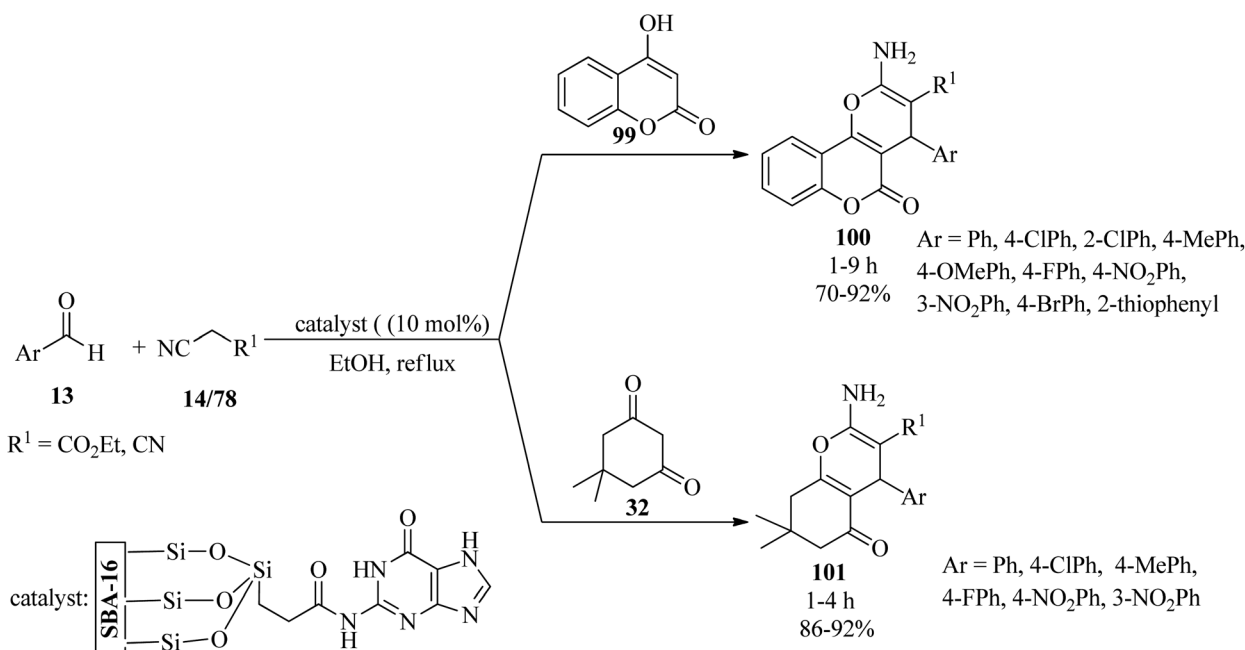




**Scheme 30** Preparation procedure of benzo[ $\alpha$ ]benzo[6,7] chromeno[2,3-c] phenazines and spiro[benzo[ $\alpha$ ]benzo[6,7] chromeno[2,3-c]phenazine] derivatives.

as guanine, piperazine, methylamine, morpholine, aniline, ethylenediamine, 3-aminopropyltriethoxysilane, and melamine to afford biodiesel (**85**) with 6–96% conversions by the *trans*-esterification reaction of soybean oil (**84**) with methanol, in 1 : 36 molar ratio, at 160 °C for 3 h (Scheme 26). According to the resulting data, guanine and melamine gave the highest and lowest yields of the product, respectively, which is ascribed to the amine basicity of the catalyst.<sup>127</sup>

Due to the remarkable pharmaceutical activities of the heterocycles possessing thiazolidin-4-one motif, such as the antitubercular, antimicrobial, anticonvulsant, anticancer, antiprotozoal, and anti-inflammatory activities,<sup>128,129</sup> Pathak and Gupta synthesized 2-iminothiazolidin-4-one derivatives (**88**) *via* the one-pot three-component annulation of amines (**45**), aryl isothiocyanates (**86**), and ethyl bromoacetate (**87**) utilizing guanine-coated SBA-16 (SBA-16@G) as an efficacious, practical, recyclable and reusable heterogeneous solid base catalyst in



**Scheme 31** Synthesis of diverse pyran-annulated heterocyclic compounds.

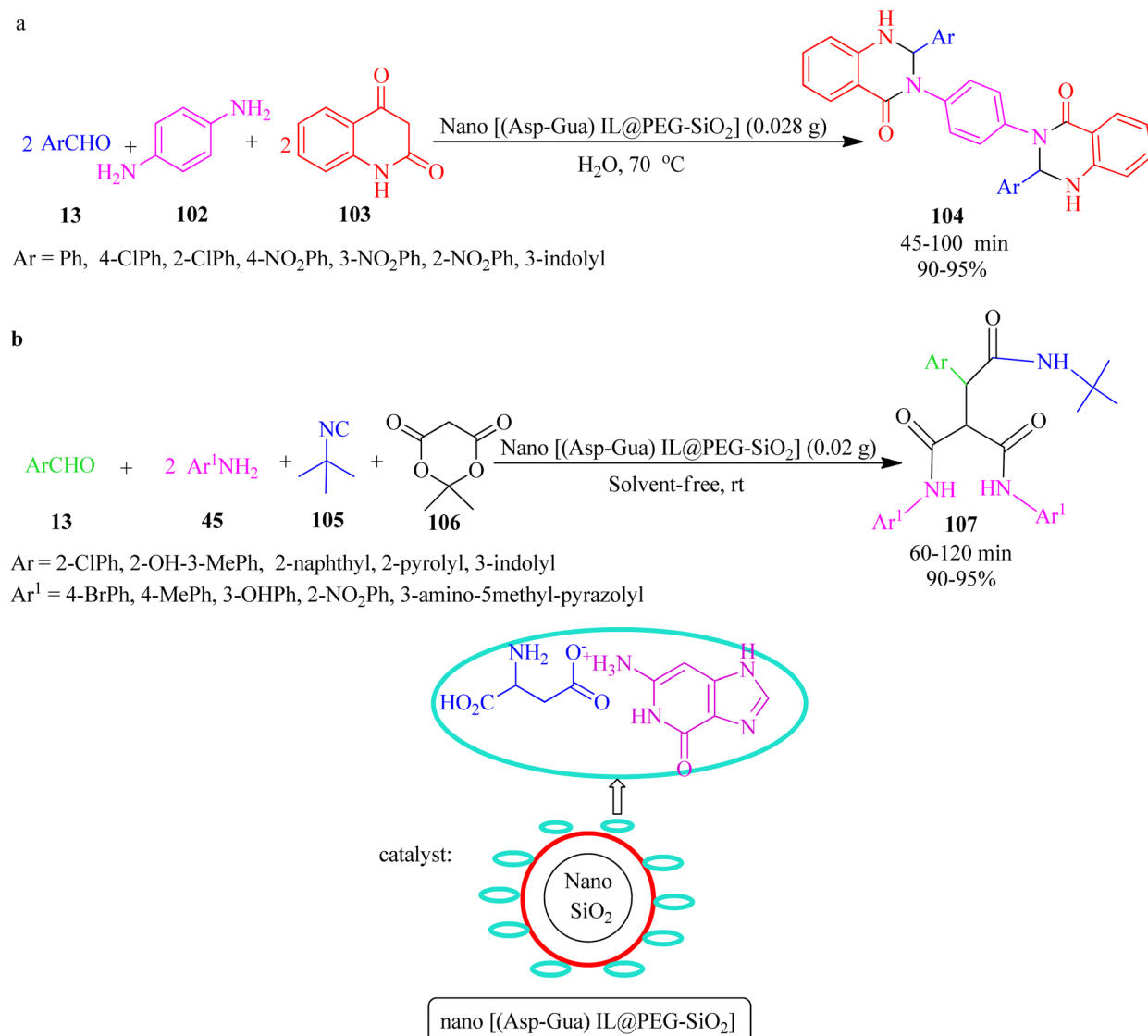


DMF at room temperature (Scheme 27). In this research, in order to probe the scope and limitations of the mentioned process, the reaction was performed using various aromatic and aliphatic amines such as aniline, benzylamines, ethylenediamine and propylamine. It was found that the reaction with benzylamines progressed faster. Remarkably, ethylenediamine and propylamine provided moderate yields (45% and 65%, respectively), while aniline gave poor yields (15%).<sup>130</sup>

In 2020, novel copper(II) ion complexes of guanine anchored on MCM-41 and SBA-15 (Cu-guanine-MCM-41 and Cu-guanine-SBA-15) channels were found to catalyze the generation of benzo[c]pyrano[3,2-*a*]phenazines (93) and bis-benzo[c]pyrano[3,2-*a*]phenazines (94) *via* the one-pot domino four-component reactions. These reactions began through the domino condensation reaction of 2-hydroxy-1,4-naphthoquinone (89) with benzene-1,2-diamine (90) in the presence of PEG at 120 °C to form phenazine (91), as the orange solid within 10 min, which was

then treated with aldehydes (13, 92) and alkylmalonates (14, 78) to achieve the adducts 93/94 (Scheme 28). The reaction works well with aldehydes containing electron-donating groups. Furthermore, malononitrile resulted in higher yields in comparison to ethyl cyanoacetate. The results showed the yield was better utilizing Cu-guanine-MCM-41 (73–89%). Some of the products revealed antimicrobial activity against the growth of *Staphylococcus aureus*.<sup>131</sup>

In 2020, Nikoorazm *et al.* obtained a novel lanthanum(III) organometallic complex through a guanine-La complex embedded in SBA-15 (La-guanine@SBA-15). The heterogeneous mesoporous nanocatalyst was utilized for the one-pot, multi-component tandem Knoevenagel condensation-Michael addition-cyclization reactions in order to prepare a series of benzo[a]pyrano[2,3-*c*]phenazines (93) *via* the domino reaction of 89, 90, 14/78, and aldehydes (13), in a 1 : 1 : 1.5 : 1 molar ratio, in refluxing ethanol in 2.5–5 h with 87–99% yields. La-



**Scheme 32** Synthesis of (a) bis(2,3-dihydroquinazolin-4(1H)-one) derivatives and (b) tricarboxamides.



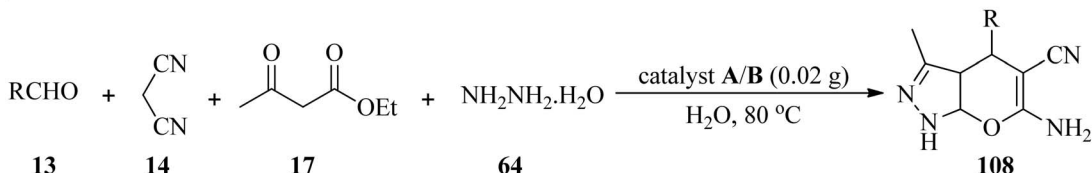
guanine@SBA-15 was also effective to obtain 4,4'-(aryl-methylene)-bis-(3-methyl-1-phenyl-1*H*-pyrazol-5-ols) derivatives (65) *via* the reaction of aldehydes (13) and 3-methyl-1-phenyl-1*H*-pyrazol-5(*H*)-one (95), in a 2:1 molar ratio (Scheme 29).<sup>132</sup> In addition, this nanocatalyst was easily recovered, using simple filtration, and reused several times without significant loss of catalytic efficiency (confirmed by SEM and FT-IR techniques). Moreover, the leaching, heterogeneity and stability of La-guanine@SBA-15 were studied using the hot filtration test and ICP techniques.

MCM-41-supported nanoscale guanine covered by Zr(IV) was prepared using the sol-gel method (Zr-guanine-MCM-41). This mesoporous nanostructure mediated the tandem chemoselective pseudo four-component reaction of 2-hydroxy-1,4-naphthoquinone (89), 90, and aldehydes (13), in a 2:1:1 molar ratio in PEG at 100 °C to produce benzo[*α*]benzo[6,7]chromeno[2,3-*c*]phenazines (96). The preparation of spiro [benzo[*α*]benzo[6,7]chromeno[2,3-*c*]phenazine] derivatives (98) was also performed through the pseudo-four-component

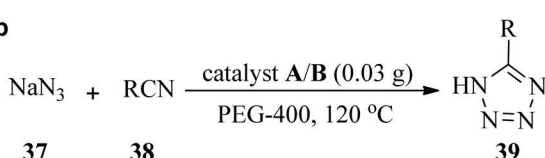
reaction of 2-hydroxy-1,4-naphthoquinone (89), 90, isatins (80)/ninhydrin (97), effectively. These reactions progressed *via* the Schiff-base condensation reaction of 89 with 90 to generate the corresponding 91, which was treated subsequently with excess amounts of 89 and 13 or 80/97 (Scheme 30). Significantly, the reactivity of aldehydes, including electron-withdrawing groups, was better. The catalytic system also progressed well with aldehydes (13) and 3-methyl-1-phenyl-5-pyrazolone (95), in a 1:2 molar ratio, to furnish bis(pyrazolyl)methanes (65) in refluxing ethanol for 10–60 min in excellent yields (83–99%). Both electron-donating and electron-withdrawing aldehydes gave the products in good yields, but the reaction time of the aryl aldehydes containing electron-donating groups was longer.<sup>133</sup>

In 2019, Gupta *et al.* synthesized guanine-functionalized mesoporous silica [SBA-16-G] with a surface area and basicity of 524 m<sup>2</sup> g<sup>-1</sup> and 3.230 mmol g<sup>-1</sup>, respectively. Its catalytic activity was explored in the synthesis of a series of pyran-annulated heterocyclic compounds 100/101 from a one-pot three-component reaction of aromatic aldehydes (13),

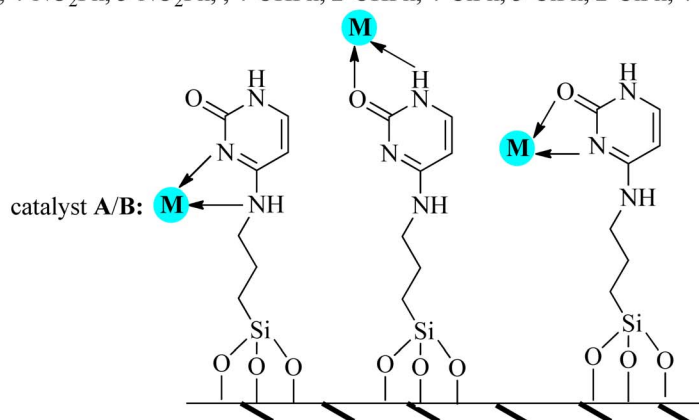
a



b

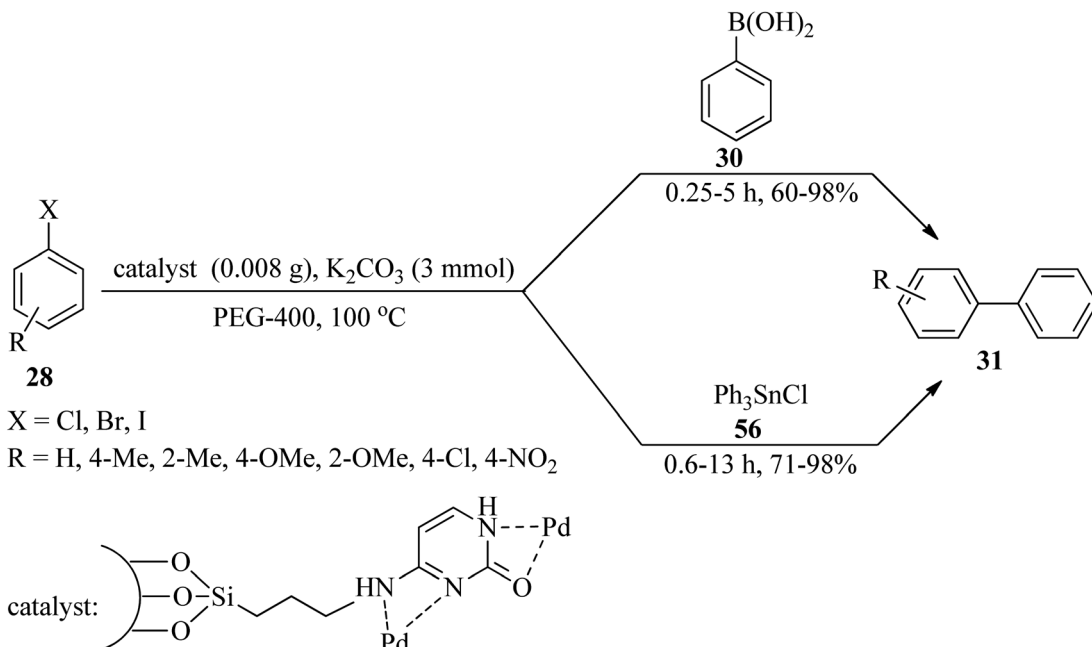


R = Ph, 4-CNPh, 2-CNPh, 4-NO<sub>2</sub>Ph, 3-NO<sub>2</sub>Ph, 4-OHPh, 2-OHPh, 4-ClPh, 3-ClPh, 2-ClPh, 4-BrPh, 4-MePh, 4-OMePh, 3,4-(OMe)<sub>2</sub>Ph



Scheme 33 Synthetic approach for (a) pyranopyrazoles and (b) 5-substituted-1*H*-tetrazoles.





Scheme 34 Biphenyl synthetic routes in the presence of HMS-CPTMS-Cy-Pd.

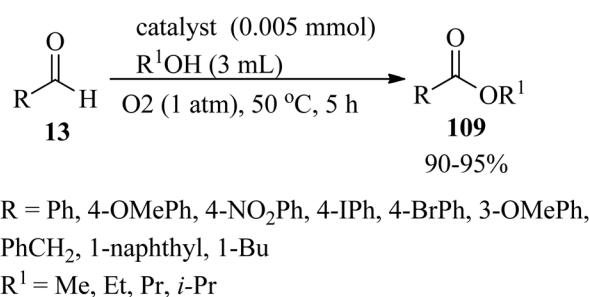
malononitrile (**14**)/ethyl cyanoacetate (**78**), and C–H activated acidic compounds (dimedone (**32**)/4-hydroxycoumarin (**99**)) (Scheme 31).<sup>134</sup> The special features of the protocol are a simple work-up procedure (no chromatography), recyclability up to four times, and the environmental acceptability of the catalyst due to metal-free catalysis.

In 2020, Nikoofar and Shahriyari prepared a novel bio-based core–shell organic–inorganic nanohybrid by embedding aspartic acid–guanine IL on the hydroxylated nanosilica surface [nano[[Asp-Gua]IL@PEG-SiO<sub>2</sub>]], as a versatile nanostructure hybrid for the synthesis of 2,3-dihydroquinazolin-4(1*H*)-one-derivatives (**104**) via the one-pot pseudo-five-component reaction of aldehydes (**13**), 1,4-benzenediamine (**102**) and isatoic anhydride (**103**) at 70 °C in aqueous media (Scheme 32a). In addition, the peptide-like

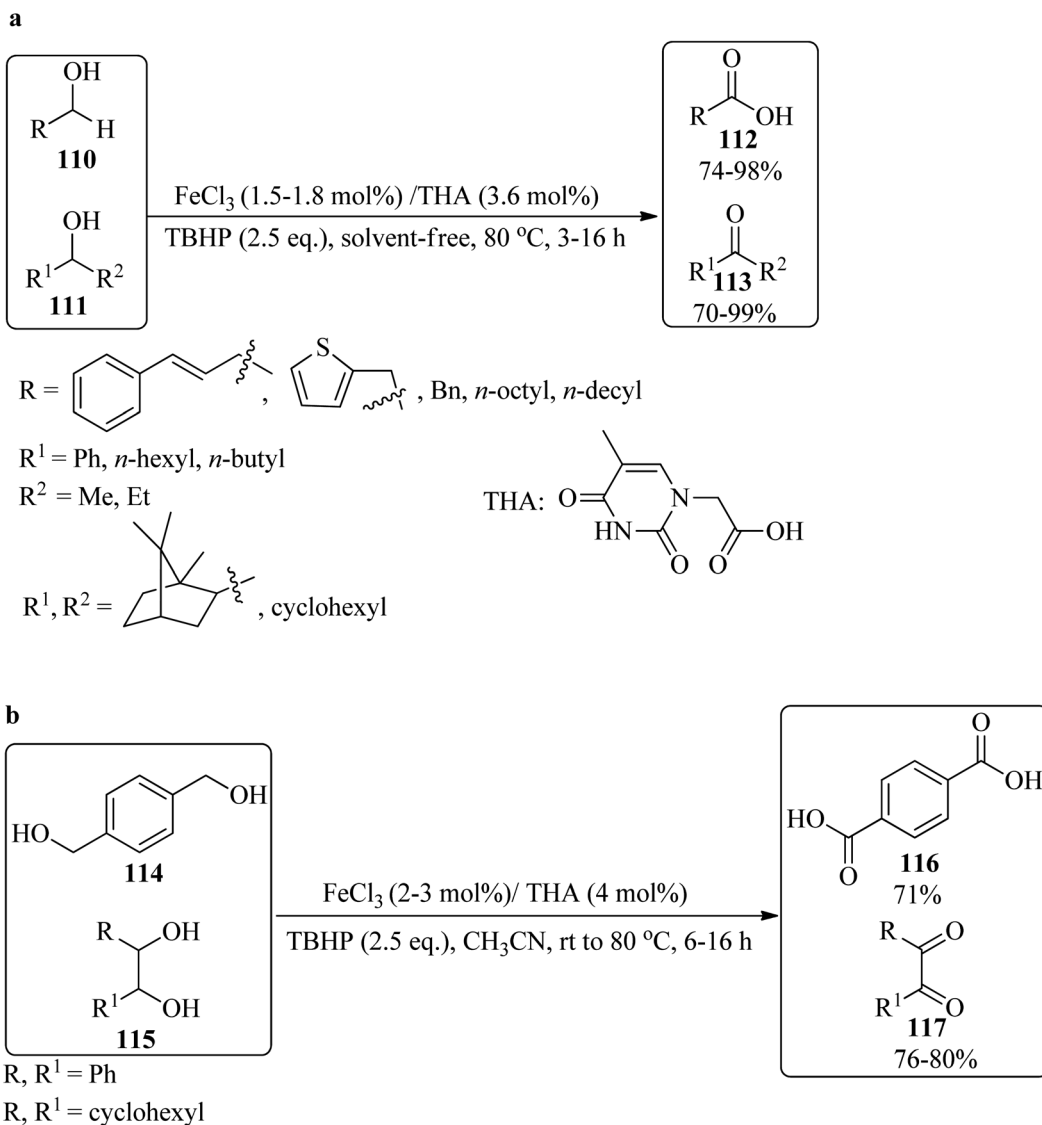
tricarboxamides (**107**) were also achieved using the pseudo-five-component condensation of aromatic aldehydes (**13**), aromatic amines (**45**), *tert*-butyl isocyanide (**105**), and Meldrum's acid (**106**) under green solventless conditions (Scheme 32b).<sup>135</sup>

#### 4. Catalytic activity of cytosine in two- and multi-component reactions

Due to the significant biological and pharmacological activities of pyranopyrazoles and tetrazoles,<sup>136–138</sup> in 2020, Nikoorazm *et al.* presented an efficient and facile method for the preparation of pyranopyrazoles (**108**) and 5-substituted-1*H*-tetrazoles (**39**) by two catalytic systems, which are copper or nickel complexes of guanine confined in the mesoporous silica (Cu-cytosine@MCM-41 and Ni-cytosine@MCM-41). Pyranopyrazoles (**108**) were produced through the four-component condensation of equimolar amounts of aldehydes (**13**), **14**, **17** and hydrazine hydrate (**64**) in water at 80 °C (Scheme 33a). On the other hand, the [3 + 2] cycloaddition of sodium azide (**37**) with nitriles (**38**) was accomplished by heating in polyethylene glycol (PEG-400) at 120 °C to give 5-substituted-1*H*-tetrazoles (**39**) (Scheme 33b). Based on the resulting data, both electron-donating and electron-withdrawing substituents on aldehydes and benzonitriles showed no significant effect on the reaction yields and the TOF. It was found that in both reactions, Cu-cytosine@MCM-41 had a great influence in decreasing the reaction time. Furthermore, the mesoporous framework of these catalysts was affirmed using nitrogen adsorption–desorption isotherms. Short reaction times, excellent yields, recyclability, and reusability of the synthesized nanocatalyst are some of the advantages of this process.<sup>139</sup>



Scheme 35 Oxidative esterification of aldehydes.



Scheme 36 Oxidation of (a) primary and secondary alcohols, and (b) diols.

In 2019, Gholamian and Hajjami synthesized and characterized a Pd-cytosine complex stabilized on functionalized hexagonal mesoporous silica (HMS-CPTMS-Cy-Pd) as a novel, recyclable, and reusable catalyst. Its catalytic activity was investigated for the preparation of biphenyls *via* two pathways: (a) the Suzuki–Miyaura cross-coupling reaction of equimolar amounts of aryl halides (**28**) with phenylboronic acid (**30**) utilizing  $K_2CO_3$  in PEG-400 at  $100\text{ }^\circ\text{C}$  gave rise to biphenyl compounds (**31**) in moderate to excellent yields (60–98%) within 0.25–5 h; (b) Stille reaction of aryl halides (**28**) and triphenyltin chloride (**56**), in a 1 : 0.5 molar ratio, under similar conditions yielded **31** (Scheme 34). The recyclability and reusability of the catalyst, experimental simplicity, short reaction times, and high yields are some of the advantages of this procedure.<sup>140</sup>

In 2021, Rajabi *et al.* constructed a cytosine palladium complex supported on ordered mesoporous silica (Pd-Cyt@SBA-15) that was utilized as a reusable nanocatalyst for the one-pot oxidative esterification of aldehydes (**13**). Diverse aliphatic,

aromatic, and unsaturated aldehydes underwent oxidative transformation to the corresponding esters (**109**) in the presence of oxygen in large turnover numbers (Scheme 35). The Pd-Cyt@SBA-15 nanocatalyst demonstrated excellent reusability and stability up to ten times without loss of significant reactivity.<sup>141</sup>

Palladium on cytosine supported on SBA-15 nanoreactors (Pd-Cyt@SBA-15) also accelerated the formation of biphenyls (**31**) *via* the Suzuki–Miyaura reaction of various aryl chlorides (**28**) with boronic acid (**30**) in the presence of  $K_2CO_3$  (1.5 mmol) base in a water/isopropanol (3 : 1) media at  $60\text{ }^\circ\text{C}$  in 88–98% yield within 6 h. Both electron-donating and electron-withdrawing aryl chlorides provided the corresponding products in excellent yields.<sup>142</sup>

In 2017, Rajabi *et al.* designed and identified novel highly-ordered periodic mesoporous silica cytosine functionalized nanomaterials (Cyt@SBA-15) for the synthesis of  $\alpha,\beta$ -unsaturated dicyanides (**55**) through the Knoevenagel condensation of



14 with aldehydes (13)/ketones (74) in ethanol at room temperature in a 1 h period with 88–99% yields. It was found that the aldehydes bearing electron-withdrawing substituents gave the related products in excellent yields, which could probably be ascribed to the higher reactivity of their carbonyl moiety. The catalytic system also indicated a good performance for less reactive ketones, in comparison with aldehydes, to furnish the corresponding compounds in 88–92% yields. Mild reaction conditions, low catalyst loading, recyclability and reusability of the catalyst, high yields, and short reaction times are some of the main advantages of this strategy.<sup>143</sup>

## 5. Catalytic activity of thymine in two- and multi-component reactions

In 2010, Al-Hunaiti *et al.* produced thymine iron(III) (THA/FeCl<sub>3</sub>) from the *in situ* reaction of anhydrous FeCl<sub>3</sub> (1.8 mol%) with thymine-1-acetate (THA, 3.6 mol%). The oxidation reaction of diverse alcohols was performed under solvent-free conditions at 80 °C by TBHP as an oxidant. The reaction was performed on various primary/secondary alcohols (110/111), which were selectively oxidized to their corresponding carboxylic acids (112)/ketones (113), respectively (Scheme 36a). On the other hand, various diols, including 1,4-dibenzylid diol (114) and internal/cyclic *vic*-diols (115) (such as diphenyl ethanediol and 1,2-cyclohexanediol), were selectively transformed to phenyl dicarboxylic acid (116) and diketones (117), respectively (Scheme 36b). Mild reaction conditions, inexpensiveness, experimental simplicity, environmentally friendly, and high yields are advantages of this strategy.<sup>144</sup>

## 6. Conclusions

In this review, several types of nanocatalysts containing nucleobases have been presented. The sections have been classified according to the reactions catalyzed by each of the bases (A, G, C, T). Based on the overall results, the employment of nucleobases in the preparation of nanocatalysts, such as the metal-free and template-free *in situ* nitrogen-doped nanosheets, led to elevated catalytic performance, for instance, good stability (mechanical and/or thermal), high selectivity, high surface-to-volume ratio, clean energy production, eco-friendly, atom efficacy, time economic exploitation, and minimum chemical waste generation (green technology). Detailed examinations in the form of a literature survey revealed that due to the numerous interaction sites in adenine and guanine, and most organic reactions were carried out by multilayered nanocatalysts, including the immobilization of the mentioned nucleobases. The authors hope that this review article will guide general readers to attain an intense interest in utilizing the four main DNA nucleobases as promoters in various organic transformations. Due to the unique characteristics of these biochemical nucleobases, their activity in the field of green chemistry and medicinal/biochemical studies will definitely expand greatly in the future.

## Data availability

No primary research results, software or code have been included and no new data were generated or analysed as part of this review.

## Conflicts of interest

There are no conflicts to declare.

## References

- 1 S. Sivakova and S. J. Rowan, Nucleobases as supramolecular motifs, *Chem. Soc. Rev.*, 2005, **34**, 9–21.
- 2 W. Saenger, *Principles of Nucleic Acid Structures*, Springer, New York, 1984.
- 3 V. N. Soyfer and V. N. Potaman, *Triple-Helical Nucleic Acids*, Springer, New York, 1995.
- 4 G. Michael Blackburn, M. J. Gait, D. Loakes and D. M. Williams, *Nucleic Acids in Chemistry and Biology*, RSC publishing, Cambridge, UK, 3rd edn, 2006.
- 5 T. L. V. Ulbricht, *Purines, Pyrimidines and Nucleotides and the Chemistry of Nucleic Acids*, Pergamon, 2016.
- 6 M. P. Callahan, Pyrimidine base, in *Encyclopedia of Astrobiology*, ed. M. Gargaud, et al., Springer, Berlin, Heidelberg, pp. , pp. 1391–1392.
- 7 J. Oro, Synthesis of adenine from ammonium cyanide, *Biochem. Biophys. Res. Commun.*, 1960, **2**, 407–412.
- 8 J. Oro and A. P. Kimball, Synthesis of purines under possible primitive earth conditions. I. adenine from hydrogen cyanide, *Arch. Biochem. Biophys.*, 1961, **94**, 217–227.
- 9 H. I. Wheeler and H. F. Merriam, On the condensation-products of the pseudothioureas: synthesis of uracil, thymine, and similar compounds, *Am. Chem. J.*, 1903, **29**, 478–492.
- 10 A. Kossel and H. Z. Steudel, Weitere untersuchungen über das cytosin, *Physiol. Chem.*, 1903, **38**, 49–59.
- 11 B. Unger, Bemerkungen zu obiger no1iz. justus, *Liebigs Ann. Chem.*, 1846, **58**, 18–20.
- 12 W. Traube, Ueber eine neue synthese des guanins und xanthins, *Ber. Dtsch. Chem. Ges.*, 1900, **33**, 1371–1383.
- 13 A. Ascoli, Ueber ein neues spaltungsprodukt des hefenucleins, *Hoppe Seyler's Z. Physiol. Chem.*, 1901, **31**, 161–214.
- 14 D. J. Brown, R. F. Evans, W. B. Cowden and M. D. Fenn, The pyrimidines, in *Chemistry of Heterocyclic Compounds*, ed. D. J. Brown, Wiley, New York, 1950, vol. 52.
- 15 K. Wang, P. Liu, D. Shi, H.-y. Zhang, Y. Zhang and J. Zhao, Nitrogen-doped carbon supported Co/Ni bimetallic catalyst for selectively reductive N-formylation of nitroso in guanine synthesis, *Catal. Lett.*, 2022, **152**, 2812–2822.
- 16 M. Robertson and S. Miller, Prebiotic Synthesis of 5-substituted uracils: A bridge between the RNA world and the DNA-protein world, *Science*, 1995, **268**, 702–705.

17 R. Saladino, C. Crestini, F. Ciciriello, G. Costanzo and E. Di Mauro, Formamide chemistry and the origin of informational polymers, *Chem. Biodivers.*, 2007, **4**, 694–720.

18 L. Petera, K. Mrazikova, L. Nejdl, K. Zemankova, M. Vaculovicova, A. Pastorek, S. Civis, P. Kubelik, A. Heays, G. Cassone, J. Sponer, M. Ferus and J. Sponer, Prebiotic route to thymine from formamide-A combined experimental-theoretical study, *Molecules*, 2021, **26**, 2248.

19 R. Saladino, G. Botta, M. Delfino and E. Di Mauro, Meteorites as catalysts for prebiotic chemistry, *Chem.-Eur. J.*, 2013, **19**, 16916–16922.

20 M. Yadav, R. Kumar and R. Krishnamurthy, Chemistry of abiotic nucleotide synthesis, *Chem. Rev.*, 2020, **120**, 4766–4805.

21 N. Kitadai and S. Maruyama, Origins of building blocks of life: A review, *Geosci. Front.*, 2018, **9**, 1117–1153.

22 K. E. Nelson, M. P. Robertson, M. Levy and S. L. Miller, Concentration by evaporation and the prebiotic synthesis of cytosine, *Origins Life Evol. Biospheres*, 2001, **31**, 221–229.

23 L. E. Orgel, Prebiotic adenine revisited: eutectics and photochemistry, *Origins Life Evol. Biospheres*, 2004, **34**, 361–369.

24 H. J. Cleaves, K. E. Nelson and S. L. Miller, The prebiotic synthesis of pyrimidines in frozen solution, *Naturwissenschaften*, 2006, **93**, 228–231.

25 C. Menor-Salvan, D. M. Ruiz-Bermejo, M. I. Guzman, S. Osuna-Esteban and S. Veintemillas-verdaguer, synthesis of pyrimidines and triazines in ice: implications for the prebiotic chemistry of nucleobases, *Chem.-Eur. J.*, 2009, **15**, 4411–4418.

26 M. Ruiz-Bermejo, C. Menor-Salvan, S. Osuna-Esteban and S. Veintemillas-Verdaguer, Prebiotic microreactors: a synthesis of purines and dihydroxy compounds in aqueous aerosol, *Origins Life Evol. Biospheres*, 2007, **37**, 123–142.

27 R. Saladino, C. Crestini, S. Pino, G. Costanzo and E. Di Mauro, Formamide and the origin of life, *Phys. Life Rev.*, 2012, **9**, 84–104.

28 R. Saladino, G. Botta, S. Pino, G. Costanzo and E. Di Mauro, Genetics first or metabolism first? The formamide clue, *Chem. Soc. Rev.*, 2012, **41**, 5526–5565.

29 H. L. Barks, R. Buckley, G. A. Grieves, E. Di Mauro, N. V. Hud and T. M. Orlando, Guanine, adenine, and hypoxanthine production in UV-irradiated formamide solutions: relaxation of the requirements for prebiotic purine nucleobase formation, *ChemBioChem*, 2010, **11**, 1240–1243.

30 R. Saladino, C. Crestini, G. Costanzo, R. Negri and E. Di Mauro, A possible prebiotic synthesis of purine, adenine, cytosine, and 4(3H)-pyrimidinone from formamide: implications for the origin of life, *Bioorg. Med. Chem.*, 2001, **9**, 1249–1253.

31 R. Saladino, U. Ciambecchini, C. Crestini, G. Costanzo, R. Negri and E. Di Mauro, One-pot  $TiO_2$ -catalyzed synthesis of nucleic bases and acyclonucleosides from formamide: implications for the origin of life, *ChemBioChem*, 2003, **4**, 514–521.

32 R. Saladino, C. Crestini, U. Ciambecchini, F. Ciciriello, G. Costanzo and E. Di Mauro, Synthesis and degradation of nucleobases and nucleic acids by formamide in the presence of montmorillonites, *ChemBioChem*, 2004, **5**, 1558–1566.

33 R. Saladino, C. Crestini, V. Neri, J. R. Brucato, L. Colangeli, F. Ciciriello, E. Di Mauro and G. Costanzo, Synthesis and degradation of nucleic acid components by formamide and cosmic dust analogues, *ChemBioChem*, 2005, **6**, 1368–1374.

34 R. Saladino, V. Neri, C. Crestini, G. Costanzo, M. Graciotti and E. Di Mauro, Synthesis and degradation of nucleic acid components by formamide and iron sulfur minerals, *J. Am. Chem. Soc.*, 2008, **130**, 15512–15518.

35 R. Saladino, V. Neri, C. Crestini, G. Costanzo, M. Graciotti and E. Di Mauro, The role of the formamide/zirconia system in the synthesis of nucleobases and biogenic carboxylic acid derivatives, *J. Mol. Evol.*, 2010, **71**, 100–110.

36 R. M. Hazen and D. A. Sverjensky, Mineral surfaces, geochemical complexities, and the origins of life, *Cold Spring Harbor Perspect. Biol.*, 2010, **2**, a002162.

37 U. Shanker, B. Bhushan and G. Bhattacharjee and Kamaluddin, Formation of nucleobases from formamide in the presence of iron oxides: Implication in chemical evolution and origin of life, *Astrobiology*, 2011, **11**, 225–233.

38 L. Nejdl, L. Petera, J. Sponer, K. Zemáková, K. Pavelcová, A. Knížek, V. Adam, M. Vaculovičová, O. Ivanek and M. Ferus, Quantum dots in peroxidase-like chemistry and formamide-based hot spring synthesis of nucleobases, *Astrobiology*, 2022, **22**, 541–551.

39 Y. Oba, Y. Takano, H. Naraoka, N. Watanabe and A. Kouchi, Nucleobase synthesis in interstellar ices, *Nat. Commun.*, 2019, **10**, 4413.

40 J. Wang, J. Gu, M. T. Nguyen, G. Springsteen and J. Leszczynski, From formamide to adenine: a self-catalytic mechanism for an abiotic approach, *J. Phys. Chem. B*, 2013, **117**, 14039–14045.

41 V. Gaded and R. Anand, Nucleobase deaminases: a potential enzyme system for new therapies, *RSC Adv.*, 2018, **8**, 23567–23577.

42 Ch. Ellouze, T. Selmane, H.-K. Kim, E. Tuite, B. Norde, K. Mortensen and M. Takahashi, Difference between active and inactive nucleotide cofactors in the effect on the DNA binding and the helical structure of RecA filament dissociation of RecA±DNA complex by inactive nucleotides, *Eur. J. Biochem.*, 1999, **262**, 88–94.

43 S. Verma, A. K. Mishra and J. Kumar, The many facets of adenine: coordination, crystal patterns, and catalysis, *Acc. Chem. Res.*, 2010, **43**, 79–91.

44 A. Conejo-García, O. Cruz-López, V. Gómez-Pérez, F. Morales, M. E. García-Rubiño, M. Kimatrai, M. C. Núñez and J. M. Campos, Synthesis of purine derivatives as scaffolds for a diversity of biological activities, *Curr. Org. Chem.*, 2010, **14**, 2463–2482.

45 D. Ramesh, B. G. Vijayakumar and T. Kannan, Therapeutic potential of uracil and its derivatives in countering



pathogenic and physiological disorders, *Eur. J. Med. Chem.*, 2020, **207**, 112801.

46 A. Singh, C. Biot, A. Viljoen, C. Dupont, L. Kremer, K. Kumar and V. Kumar, 1H-1,2,3-triazole-tethered uracil-ferrocene and uracil-ferrocenylchalcone conjugates: Synthesis and antitubercular evaluation, *Chem. Biol. Drug Des.*, 2017, **89**, 856–861.

47 L. Harmse, N. Gray, P. Schultz, S. Leclerc, D. C. Meijer and I. Havli, Structure-activity relationships and inhibitory effects of various purine derivatives on the in vitro growth of *Plasmodium falciparum*, *Biochem. Pharmacol.*, 2001, **62**, 341–348.

48 L. Meijer and E. Raymond, Roscovitine and other purines as kinase inhibitors. From starfish oocytes to clinical trials, *Acc. Chem. Res.*, 2003, **36**, 417–425.

49 A. E. J. Yssel, J. Vanderleyden and H. P. Steenackers, Repurposing of nucleoside- and nucleobase-derivative drugs as antibiotics and biofilm inhibitors, *J. Antimicrob. Chemother.*, 2017, **72**, 2156–2170.

50 D. Ramesh, A. K. Mohanty, A. De, B. G. Vijayakumar, A. Sethumadhavan, S. K. Muthuvel, M. Mani and T. Kannan, Uracil derivatives as HIV-1 capsid protein inhibitors: design, in silico, in vitro and cytotoxicity studies, *RSC Adv.*, 2022, **12**, 17466–17480.

51 P. A. Bonnet and R. K. Robins, Modulation of leukocyte genetic expression by novel purine nucleoside analogs. A new approach to antitumor and antiviral agents, *J. Med. Chem.*, 1993, **36**, 635–653.

52 D. Ramesh, B. G. Vijayakumar and T. Kannan, Advances in nucleoside and nucleotide analogues in tackling human immunodeficiency virus and hepatitis virus infections, *ChemMedChem*, 2021, **16**, 1403–1419.

53 C. Wang, Z. Song, H. Yu, K. Liu and X. Man, Adenine: an important drug scaffold for the design of antiviral agents, *Acta Pharm. Sin. B*, 2015, **5**, 431–441.

54 E. Badawey and T. Kappe, Synthesis of some new imidazo [1,2-a]pyrimidin-5(1H)-ones as potential antineoplastic agents, *J. Heterocycl. Chem.*, 1995, **32**, 1003–1006.

55 D. K. Tosh, K. A. Jacobson and L. S. Jeong, Nucleoside-based A3 adenosine receptor antagonists as drug candidates, *Drugs Future*, 2009, **34**, 0043.

56 G. Nogueira, A. Favrelle, M. Bria, J. P. Ramalho, P. J. Mendes, A. Valente and P. Zinck, Adenine as an organocatalyst for the ring-opening polymerization of lactide: scope, mechanism and access to adenine-functionalized polylactide, *React. Chem. Eng.*, 2016, **1**, 508–520.

57 Y. Wang, S. Zhao, Y. Zhang, W. Chen, S. Yuan, Y. Zhou and Z. Huang, Synthesis of graphitic carbon nitride with large specific surface area via copolymerizing with nucleobases for photocatalytic hydrogen generation, *Appl. Surf. Sci.*, 2019, **463**, 1–8.

58 H. Yang and W. Xi, Nucleobase-containing polymers: structure, synthesis, and applications, *Polymers*, 2017, **9**, 666.

59 F. Bahrami, F. Panahi, F. Daneshgar, R. Yousefi, M. B. Shahsavani and A. Khalafi-Nezhad, Synthesis of new  $\alpha$ -aminophosphonate derivatives incorporating benzimidazole, theophylline and adenine nucleobases using Leysteine functionalized magnetic nanoparticles (LCMNP) as magnetic reusable catalyst: Evaluation of their anticancer properties, *RSC Adv.*, 2016, **6**, 5915–5924.

60 F. De Castro, E. Stefano, F. P. Fanizzi, R. Di Corato, P. Abdalla, F. Luchetti, M. G. Nasoni, R. Rinaldi, M. Magnani, M. Benedetti and A. Antonelli, Compatibility of nucleobases containing Pt(II) complexes with red blood cells for possible drug delivery applications, *Molecules*, 2023, **28**, 6760.

61 X. Tan, F. Jia, P. Wang and K. Zhang, Nucleic Acid-based drug delivery strategies, *J. Controlled Release*, 2020, **323**, 240–252.

62 M.-A. Morikawa, M. Yoshihara, T. Endo and N. Kimizuka, ATP as building blocks for the self-assembly of excitonic nanowires, *J. Am. Chem. Soc.*, 2005, **127**, 1358–1359.

63 A. Terrón, J. J. Fiol, A. García-Raso, M. Barceló-Olivier and V. Moreno, Biological recognition patterns implicated by the formation and stability of ternary metal ion complexes of low-molecular-weight formed with amino acid/peptides and nucleobases/nucleosides, *Coord. Chem. Rev.*, 2007, **251**, 1973–1986.

64 F. Pu, J. Ren and X. Qu, Nucleobases, nucleosides, and nucleotides: versatile biomolecules for generating functional nanomaterials, *Chem. Soc. Rev.*, 2018, **47**, 1285–1306.

65 L. Stefan and D. Monchaud, Applications of guanine quartets in nanotechnology and chemical biology, *Nat. Rev. Chem.*, 2019, **3**, 650–668.

66 M. Hocek and M. Fojta, Nucleobase modification as redox DNA labelling for electrochemical Detection, *Chem. Soc. Rev.*, 2011, **40**, 5802–5814.

67 Y. Xing, Y. Zhang, X. Zhu, C. Wang, T. Zhang, F. Cheng, J. Qu and W. J. G. M. Peijnenburg, A highly selective and sensitive electrochemical sensor for tetracycline resistant genes detection based on the non-covalent interaction of graphene oxide and nucleobase, *Sci. Total Environ.*, 2024, **906**, 167615.

68 J. Zhou, H. Han and J. Liu, Nucleobase, nucleoside, nucleotide, and oligonucleotide coordinated metal ions for sensing and biomedicine applications, *Nano Res.*, 2022, **15**, 71–84.

69 B. Huang, X. Hu, Y. Liu, W. Qi and Z. Xie, Biomolecule-derived N/S co-doped CNT-graphene hybrids exhibiting excellent electrochemical activities, *J. Power Sources*, 2019, **414**, 408–417.

70 B. Huang, Y. Liu, X. Huang and Z. Xie, Multiple heteroatom-doped few-layer carbons for the electrochemical oxygen reduction reaction, *J. Mater. Chem. A*, 2018, **6**, 22277–22286.

71 X. Du, J. Zhou and B. Xu, Supramolecular Hydrogels made of basic biological building blocks, *Chem.-Asian J.*, 2014, **9**, 1446–1472.

72 S. Sivakova and S. J. Rowan, Nucleobases as supramolecular motifs, *Chem. Soc. Rev.*, 2005, **34**, 9–21.

73 J. Pascual-Colino, G. Beobide, O. Castillo, P. Lodewyckx, A. Luque, S. Pérez-Yáñez, P. Román and L. F. Velasco,



Adenine nucleobase directed supramolecular architectures based on ferrimagnetic heptanuclear copper(II) entities and benzenecarboxylate anions, *J. Inorg. Biochem.*, 2020, **202**, 110865.

74 Y. Tian, H. Wu, A. Hanif, Y. Niu, Y. Yin, Y. Gu, Z. Chen, Q. Gu, Y. H. Ng, J. Shang, L. Li and M. Liu, N-doped graphitic carbon encapsulating cobalt nanoparticles derived from novel metal-organic frameworks for electrocatalytic oxygen evolution reaction, *Chin. Chem. Lett.*, 2023, **34**, 108056.

75 J. Chen, T. Gong, Q. Hou, J. Li, L. Zhang, D. Zhao, Y. Luo, D. Zheng, T. Li, S. Sun, Z. Cai, Q. Liu, L. Xie, M. Wu, A. A. Alshehri and X. Sun, Co/N-doped carbon nanospheres derived from an adenine-based metal organic framework enabled high-efficiency electrocatalytic nitrate reduction to ammonia, *Chem. Commun.*, 2022, **58**, 13459–13462.

76 H. Guo, Q. Feng, J. Zhu, J. Xu, Q. Li, S. Liu, K. Xu, C. Zhang and T. Liu, Cobalt nanoparticle-embedded nitrogen-doped carbon/carbon nanotube frameworks derived from metal-organic framework for tri-functional ORR, OER and HER electrocatalysis, *J. Mater. Chem. A*, 2019, **7**, 3664–3672.

77 B. Huang, Y. Li, X. Guan and Z. Xie, Nucleobases-derived carbon materials: Synthesis and application in heterogeneous catalysis, *FlatChem*, 2022, **35**, 100415.

78 S. A. Abbas, J. T. Song, Y. C. Tan, K. M. Nam, J. Oh and K.-D. Jung, Synthesis of nickel single-atom catalyst based on ni-n4-xcx active sites for highly efficient CO<sub>2</sub> reduction utilizing gas diffusion electrode, *ACS Appl. Energy Mater.*, 2020, **3**, 8739–8745.

79 Y. Liu, X. Hu, B. Huang and Z. Xie, Surface engineering of Rh catalysts with N/S-codoped carbon nanosheets toward high-performance hydrogen evolution from seawater, *ACS Sustain. Chem. Eng.*, 2019, **7**, 18835–18843.

80 Y. Kobayashi, R. Tanahashi, Y. Yamaguchi, N. Hatae, M. Kobayashi, Y. Ueno and M. Yoshimatsu, Ni-Pd catalyzed cyclization of sulfanyl 1,6-dynes: synthesis of 1'-homonucleoside analogs, *J. Org. Chem.*, 2017, **82**, 2436–2449.

81 M. Ma, L. Liu, H. Xu, X. Yang, H. Wang, X. Lu, P. Yang, P. Wu and L. Liao, Molten salt-mediated synthesis of porous N-doped carbon as an efficient ORR electrocatalyst for zinc-air batteries, *New J. Chem.*, 2023, **47**, 2279–2285.

82 B. Huang, Y. Liu, M. Xia, J. Qiu and Z. Xie, Building microsphere–nanosheet structures in N-doped carbon to improve its performance in the oxygen reduction reaction and vanadium redox flow batteries, *Sustainable Energy Fuels*, 2020, **4**, 559–570.

83 B. Huang, Y. Liu and Z. Xie, Two dimensional nanocarbons from biomass and biological molecules: Synthetic strategies and energy related applications, *J. Energy Chem.*, 2021, **54**, 795–814.

84 B. Huang, Y. Liu, Q. Wei and Z. Xie, Three-dimensional mesoporous graphene-like carbons derived from biomolecule exhibiting high-performance oxygen reduction activity, *Sustainable Energy Fuels*, 2019, **3**, 2809–2818.

85 B. Huang, Y. Liu, Q. Guo, Y. Fang, M.-M. Titirici, X. Wang and Z. Xie, Porous carbon nanosheets from biological nucleobase precursor as efficient pH-independent oxygen reduction electrocatalyst, *Carbon*, 2020, **156**, 179–186.

86 Y. Liu, B. Huang, X. Zhang, X. Huang and Z. Xie, In-situ fabrication of nitrogen-doped carbon nanosheets containing highly dispersed single iron atoms for oxygen reduction reaction, *J. Power Sources*, 2019, **412**, 125–133.

87 Y. Li, F. Hou, X. Sun, Z. Xiao, X. Zhang and G. Li, Toward an understanding of capping molecules on Pt nanoparticles for hydrogenation: the key role of hydroxyl groups, *ChemistrySelect*, 2019, **4**, 3505–3514.

88 Q. Li, Y. Chen, S. Bai, X. Shao, L. Jiang and Q. Li, Immobilized lipase in bio-based metal-organic frameworks constructed by biomimetic mineralization: A sustainable biocatalyst for biodiesel synthesis, *Colloids Surf. B*, 2020, **188**, 110812.

89 F. Bruston, J. Vergne, L. Grajcar, B. Drahi, R. Calvayrac, M.-H. Baron and M.-C. Maurel, Copper-adenine catalyst for O<sub>2</sub> production from H<sub>2</sub>O<sub>2</sub>, *Biochem. Biophys. Res. Commun.*, 1999, **263**, 672–677.

90 R. Li, X. Zhang, C. Zhang, J. Lu, J.-C. Wang, C.-X. Cui, X. Yang, F. Huang, J.-X. Jiang and Y. Zhang, Adenine-functionalized conjugated polymer as an efficient photocatalyst for hydrogen evolution from water, *Int. J. Hydrogen Energy*, 2022, **47**, 29771–29780.

91 R. M. C. Dawson, D. C. Elliott, W. H. Elliott and K. M. Jones, *Data for Biochemical Research*, Oxford University Press, Oxford, 3rd edn, 1986.

92 K. Karrouchi, S. Radi, Y. Ramli, J. Taoufik, Y. N. Mabkhot, F. A. Al-aizari and M. Ansar, Synthesis and pharmacological activities of pyrazole derivatives: A review, *Molecules*, 2018, **23**, 134.

93 F. E. Bennani, L. Doudach, Y. Cherrah, Y. Ramli, Kh. Karrouchi, M. Ansar and M. E. A. Faouzi, Overview of recent developments of pyrazole derivatives as an anticancer agent in different cell line, *Bioorg. Chem.*, 2020, **97**, 103470.

94 M. A. Elsherif, A. S. Hassan, G. O. Moustafa, H. M. Awad and N. M. Morsy, Antimicrobial evaluation and molecular properties prediction of pyrazolines incorporating benzofuran and pyrazole moieties, *J. Appl. Pharm. Sci.*, 2020, **10**, 37–43.

95 O. Ebenezer, M. Shapi and J. A. Tuszyński, A review of the recent development in the synthesis and biological evaluations of pyrazole derivatives, *Biomedicines*, 2022, **10**, 1124.

96 E. Ahmadi, A. Khazaei and T. Akbarpour,  $[Fe_3O_4@CQD@Si(OEt)(CH_2)_3NH@CC@Ad@SO_3H]^{+}Cl^-$ : As a new, efficient, magnetically separable and reusable heterogeneous solid acid catalyst for the synthesis of 5-amino-1,3-diphenyl-1H-pyrazole 4-carbonitril and pyrano [2,3-c]pyrazole derivatives, *Res. Chem. Intermed.*, 2023, **49**, 2099–2122.

97 Z. Sadri, F. K. Behbahani and E. Keshmirizadeh, One-pot multicomponent synthesis of 2,6-diamino-4-arylpypyridine-3,5-dicarbonitriles using prepared nanomagnetic



Fe<sub>3</sub>O<sub>4</sub>@SiO<sub>2</sub>@(CH<sub>2</sub>)<sub>3</sub>NHCOadenine sulfonic acid, *Inorg. Nano-Met. Chem.*, 2022, **54**, 839–848.

98 Z. Sadri, F. K. Behbahani and E. Keshmirizadeh, Synthesis and characterization of a novel and reusable adenine based acidic nanomagnetic catalyst and its application in the preparation of 2-substituted-2,3-dihydro-1H-perimidines under ultrasonic irradiation and solvent-free condition, *Polycyclic Aromat. Compd.*, 2023, **43**, 1898–1913.

99 C. Feng, S. Qiao, Y. Guo, Y. Xie, L. Zhang, N. Akram, S. Li and J. Wang, Adenine-assisted synthesis of functionalized F-Mn-MOF-74 as an efficient catalyst with enhanced catalytic activity for the cycloaddition of carbon dioxide, *Colloids Surf., A*, 2020, **597**, 124781.

100 Y. Rachuri, J. F. Kurisingal, R. K. Chitumalla, S. Vuppala, Y. Gu, J. Jang, Y. Choe, E. Suresh and D.-W. Park, Adenine-based Zn(II)/Cd(II) metal-organic frameworks as efficient heterogeneous catalysts for facile CO<sub>2</sub> fixation into cyclic carbonates: a DFT-supported study of the reaction mechanism, *Inorg. Chem.*, 2019, **58**, 11389–11403.

101 N. Guha, S. Krishnan, S. Gupta and D. K. Rai, Adenine-Functionalized Dendritic fibrous nanosilica as bifunctional catalyst for CO<sub>2</sub> fixation into cyclic carbonate, *ChemNanoMat*, 2023, **9**, e202200519.

102 R. Srivastava, D. Srinivas and P. Ratnasamy, CO<sub>2</sub> activation and synthesis of cyclic carbonates and alkyl/aryl carbamates over adenine-modified Ti-SBA-15 solid catalysts, *J. Catal.*, 2005, **233**, 1–15.

103 A. Ghorbani-Choghamarani, P. Moradi and B. Tahmasbi, Modification of boehmite nanoparticles with Adenine for the immobilization of Cu(II) as organic-inorganic hybrid nanocatalyst in organic reactions, *Polyhedron*, 2019, **163**, 98–107.

104 T. Tamoradi, A. Ghorbani-Choghamarani and M. Ghadermazi, Synthesis of new zirconium complex supported on MCM-41 and its application as an efficient catalyst for synthesis of sulfides and the oxidation of sulfur containing compounds, *Appl. Organomet. Chem.*, 2018, **32**, e4340.

105 T. Tamoradi, M. Ghadermazi and A. Ghorbani-Choghamarani, Ni(II)-Adenine complex coated Fe<sub>3</sub>O<sub>4</sub> nanoparticles as high reusable nanocatalyst for the synthesis of polyhydroquinoline derivatives and oxidation reactions, *Appl. Organomet. Chem.*, 2018, **32**, e3974.

106 T. Tamoradi, A. Ghorbani-Choghamarani and M. Ghadermazi, Fe<sub>3</sub>O<sub>4</sub>-Adenine-Zn: as a novel, green and magnetically recoverable catalyst for the synthesis of 5-substituted tetrazoles and oxidation of sulfur containing compounds, *New J. Chem.*, 2017, **41**, 11714–11721.

107 M. Nikoorazm, A. Ghorbani-Choghamarani, M. Khanmoradi and P. Moradi, Synthesis and characterization of Cu(II)-Adenine-MCM-41 as stable and efficient mesoporous catalyst for the synthesis of 5-substituted 1H-tetrazoles and 1H-indazolo[1,2-b]phthalazine-triones, *J. Porous Mater.*, 2018, **25**, 1831–1842.

108 V. Khorram Abadi, D. Habibi, S. Heydari and M. M. Gilan, An adenine-based palladium complex: a capable heterogeneous magnetic nano-catalyst for the green synthesis of the ureas in aqueous media, *J. Iran. Chem. Soc.*, 2023, **20**, 1985–1996.

109 P. Goswami and B. Das, Adenine as aminocatalyst for green synthesis of diastereoselective Mannich products in aqueous medium, *Tetrahedron Lett.*, 2009, **50**, 2384–2388.

110 W. Notz, F. Tanaka and C. F. Barbas, Enamine-based organocatalysis with proline and diamines: the development of direct catalytic asymmetric Aldol, Mannich, Michael, and Diels-Alder reactions, *Acc. Chem. Res.*, 2004, **37**, 580–591.

111 B. Tahmasbi, A. Ghorbani-Choghamarani and P. Moradi, Palladium fabricated on boehmite as an organic-inorganic hybrid nanocatalyst for the C-C cross coupling and chomoselective cycloaddition reactions, *New J. Chem.*, 2020, **44**, 3717–3727.

112 X. Wang, X. Liang, P. Geng and Q. Li, Recent advances in selective hydrogenation of cinnamaldehyde over supported metal-based catalysts, *ACS Catal.*, 2020, **10**, 2395–2412.

113 X. Lan and T. Wang, Highly selective catalysts for the hydrogenation of unsaturated aldehydes: a review, *ACS Catal.*, 2020, **10**, 2764–2790.

114 P. Gallezot and D. Richard, Selective hydrogenation of  $\alpha,\beta$ -unsaturated aldehydes, *Catal. Rev.*, 1998, **40**, 81–126.

115 Y. Tang, K. Cui, Y. Li, H. Li, Y. Lei, J. Chen, W. Xiong and G. Yuan, Mild-temperature chemoselective hydrogenation of cinnamaldehyde over amorphous Pt/Fe-Asp-A nanocatalyst with enhanced stability, *Colloids Surf., A*, 2022, **654**, 130106.

116 W. She, J. Wang, X. Li, J. Li, G. Mao, W. Li and G. Li, Bimetallic CuZn-MOFs derived Cu-ZnO/C catalyst for reductive amination of nitroarenes with aromatic aldehydes tandem reaction, *Appl. Surf. Sci.*, 2021, **569**, 151033.

117 Sh. Zhang, H. He, F. Sun, N. Zhao, J. Du, Q. Pan and G. Zhu, A novel adenine-based zinc(II) metal-organic framework featuring the Lewis basic sites for heterogeneous catalysis, *Inorg. Chem. Commun.*, 2017, **79**, 55–59.

118 T. Tamoradi, M. Ghadermazi and A. Ghorbani-Choghamarani, SBA-15@adenine-Pd: a novel and green heterogeneous nanocatalyst in Suzuki and Stille reactions and synthesis of sulfides, *J. Porous Mater.*, 2019, **26**, 121–131.

119 M. M. Heravi, S. J. Mahdizade, M. Esfandiari and E. Hashemi, Experimental and computational studies on catalytic activity of novel adenine-based nano Cu(I) polymers in regioselective synthesis of 1,4-disubstituted 1,2,3-triazoles, *J. Inorg. Organomet. Polym.*, 2018, **28**, 767–776.

120 B. Chowhan, M. Gupta and N. Sharma, Fabrication and characterization of adenine-grafted carbonmodified amorphous ZnO with enhanced catalytic activity, *Appl. Organomet. Chem.*, 2020, e6013.

121 G. Wang, P. Wang, X. Zhang, Q.-H. Wei, S. Wu and Z. Xie, Nucleobase derived boron and nitrogen co-doped carbon



nanosheets as efficient catalyst for selective oxidation and reduction reactions, *Nanoscale*, 2020, **12**, 7797–7803.

122 S. Z. Alizadeh, B. Karimi and H. Vali, From deep eutectic solvents to nitrogen-rich ordered mesoporous carbons: a powerful host for the immobilization of palladium nanoparticles in the aerobic oxidation of alcohols, *ChemCatChem*, 2022, **14**, e202101621.

123 S. Li, Y. Ke, X. Zhang, S. Wu, Y. Chen and Z. Xie, Guanine-derived nitrogen-doped carbon nanosheets for selective oxidation of benzyl alcohol, *Diam. Relat. Mater.*, 2023, **132**, 109642.

124 J. C. Ng, C. Y. Tan, B. H. Ong, A. Matsuda, W. J. Basirun, W. K. Tan, R. Singh and B. K. Yap, Novel palladium-guanine-reduced graphene oxide nanocomposite as efficient electrocatalyst for methanol oxidation reaction, *Mater. Res. Bull.*, 2019, **112**, 213–220.

125 X. Hu, Y. Chen, B. Huang, Y. Liu, H. Huang and Z. Xie, Pd-supported N/S-codoped graphene-like carbons boost quinoline hydrogenation activity, *ACS Sustainable Chem. Eng.*, 2019, **7**, 11369–11376.

126 D. Saberi, M. Bashkar, A. Rezaei, Z. Azizi and K. Niknam, Guanine base stabilized on the magnetic nanoparticles as recyclable catalyst “on water” for the synthesis of spirooxindole derivatives, *J. Organomet. Chem.*, 2021, **948**, 121912.

127 F. Farzaneh, Z. Mohammadi and Z. Azarkamanzad, Immobilized different amines on modified magnetic nanoparticles as catalyst for biodiesel production from soybean oil, *J. Iran. Chem. Soc.*, 2018, **15**, 1625–1632.

128 N. Trotsko, Antitubercular properties of thiazolidin-4-ones: A review, *Eur. J. Med. Chem.*, 2021, **215**, 113266.

129 D. Mech, A. Kurowska and N. Trotsko, The Bioactivity of thiazolidin-4-ones: A short review of the most recent studies, *Int. J. Mol. Sci.*, 2021, **2**, 11533.

130 R. Gupta and D. D. Pathak, Synthesis of 2-iminothiazolidin-4-ones using guanine functionalized SBA-16 as a solid base catalyst, *Tetrahedron Lett.*, 2021, **85**, 153497.

131 M. Nikoorazm and M. Khanmoradi, Application of Cu(II)-guanine complexes anchored on SBA-15 and MCM-41 as efficient nanocatalysts for one-pot, four-component domino synthesis of phenazine derivatives and investigation of their antimicrobial behavior, *Catal. Lett.*, 2020, **150**, 2823–2840.

132 M. Nikoorazm, M. Khanmoradi and M. Mohammadi, Guanine-La complex supported onto SBA-15: a novel efficient heterogeneous mesoporous nanocatalyst for one-pot, multi-component tandem Knoevenagel condensation-Michael addition-cyclization reactions, *Appl. Organomet. Chem.*, 2020, e5504.

133 M. Nikoorazm, M. Mohammadi and M. Khanmoradi, Zirconium@guanine@MCM-41 nanoparticles: An efficient heterogeneous mesoporous nanocatalyst for one-pot, multicomponent tandem Knoevenagel condensation-Michael addition-cyclization Reactions, *Appl. Organomet. Chem.*, 2020, **34**, e5704.

134 R. Gupta, S. Layek and D. D. Pathak, Synthesis and characterization of guanine-functionalized mesoporous silica [SBA-16-G]: a metal-free and recyclable heterogeneous solid base catalyst for synthesis of pyran-annulated heterocyclic compounds, *Res. Chem. Intermed.*, 2019, **5**, 1619–1637.

135 K. Nikoofar and F. Shahriyari, Novel bio-based core-shell organic-inorganic nanohybrid from embedding aspartic acid-guanine ionic liquid on the hydroxylated nano silica surface (nano [(Asp-Gua) IL@PEG-SiO<sub>2</sub>]): A versatile nanostructure for the synthesis of bis(2,3-dihydroquinazolin-4(1H)-one) derivatives and tricarboxamides under green media, *Polyhedron*, 2020, **179**, 114361.

136 C. G. Neochoritis, T. Zhao and A. Dömling, Tetrazoles via multicomponent reactions, *Chem. Rev.*, 2019, **119**, 1970–2042.

137 I. Sarosh, K. Shumaila, A. Aliza, A. Shazia, Kh. Ansa, M. G. Mark and A. N. Muhammad, An overview of synthetic routes of pharmaceutically important pyranopyrazoles, *Curr. Med. Chem.*, 2022, **29**, 6288–6333.

138 C. Gao, L. Chang, Z. Xu, X.-F. Yan, C. Ding, F. Zhao, X. Wu and L.-S. Feng, Recent advances of tetrazole derivatives as potential anti-tubercular and anti-malarial agents, *Eur. J. Med. Chem.*, 2019, **163**, 404–412.

139 M. Nikoorazm, B. Tahmasbi, S. Gholami and P. Moradi, Copper and nickel immobilized on cytosine@MCM-41: as highly efficient, reusable and organic-inorganic hybrid nanocatalysts for the homoselective synthesis of tetrazoles and pyranopyrazoles, *Appl. Organomet. Chem.*, 2020, **34**, e5919.

140 F. Gholamian and M. Hajjami, Synthesis of Pd immobilized on functionalized hexagonal mesoporous silica (HMS-CPTMS-Cy-Pd) for coupling Suzuki-Miyaura and Stille reactions, *Polyhedron*, 2019, **170**, 649–658.

141 F. Rajabi, C. H. Chia, M. Sillanpää, L. G. Voskressensky and R. Luque, Cytosine palladium complex supported on ordered mesoporous silica as highly efficient and reusable nanocatalyst for one-pot oxidative esterification of aldehydes, *Catalysts*, 2021, **11**, 1482.

142 F. Rajabi, F. Fayyaza, R. Bandyopadhyay, F. Ivars-Barcelo, A. R. Puente-Santiago and R. Luque, Cytosine palladium hybrid complex immobilized on SBA-15 as efficient heterogeneous catalyst for the aqueous Suzuki-Miyaura coupling, *ChemistrySelect*, 2018, **3**, 6102–6106.

143 F. Rajabi, F. Fayyaz and R. Luque, Cytosine-functionalized SBA-15 mesoporous nanomaterials: synthesis, characterization and catalytic applications, *Microporous Mesoporous Mater.*, 2017, **253**, 64–70.

144 A. Al-Hunaiti, T. Niemi, A. Sibaoui, P. Pihko, M. Leskelä and T. Repo, Solvent free oxidation of primary alcohols and diols using thymine iron(III) catalyst, *Chem. Commun.*, 2010, **46**, 9250–9252.

